AFOSR-TR-97

0358

REPORT DOCUMENTATION PAGE

1. AGENCY USE ONLY (Leave blank)	2. REPORT DATE 7/15/97	3. REPORT TYPE AND DATES COVERED FINAL REPORT 01 Jun 94 – 31 May 97

4. TITLE AND SUBTITLE Development of Advanced Electronic Materials and Devices for Ultra-Low 1/f Noise and Low Leakage Current Applications	5. FUNDING NUMBERS 61102F 2305/CS

6. AUTHOR(S)

Peter H. Handel

7. PERFORMING ORGANIZATION NAME(S) AND ADDRESS(ES) University of Missouri-St. Louis 8001 Natural Bridge Rd. St. Louis, MO 63121	8. PERFORMING ORGANIZATION REPORT NUMBER

9. SPONSORING/MONITORING AGENCY NAME(S) AND ADDRESS(ES) AFOSR / NE Bldg. 410 Bolling Air Force Base Washington, DC 20332-6448	10. SPONSORING/MONITORING AGENCY REPORT NUMBER F49620-94-1-0342

11. SUPPLEMENTARY NOTES

12a. DISTRIBUTION/AVAILABILITY STATEMENT Approved for Public Release Distribution Unlimited	12b. DISTRIBUTION CODE

13. ABSTRACT (Maximum 200 words)

This report contains practical applications of the Quantum 1/f Effect, theory development, and contributions not directly based on quantum 1/f noise. The application to quartz resonators was improved by the inclusion of crystal defects in the calculation, and was generalized to the case of low-Q and SAW devices. The generalization is important, introducing the notion of incoherence between quantum 1/f fluctuations of the phonon loss rate in various regions of the crystal.

The applications also include calculation of quantum 1/f noise in gallium nitride. It is 3-10 times lower in GaN than in GaAs.

The theory was reformulated on the basis of the new negative conditional quantum entropy concept explaining the apparent entropy production in 1/f noise by simultaneous production of negative-entropy soft photon states. A long-standing conceptual difficulty is eliminated on this basis. Of tremendous importance is the discovery during this grant of a new method connecting the coherent and conventional quantum 1/f effects. A mass distribution was found, which allows to find the quantum 1/f noise in general.

A method of gate current suppression in HFET and a two-dimensional all-optical TDM system were studied.

14. SUBJECT TERMS Quantum 1/f Noise Theory, 1/f Noise, Electronic Noise in Semiconductor Devices, Quantum 1/f Effect, Bipolar Transistors, Noise in Ultrasmall Devices, Chaos, Nonlinear Dynamics		15. NUMBER OF PAGES
		16. PRICE CODE

17. SECURITY CLASSIFICATION OF REPORT	18. SECURITY CLASSIFICATION OF THIS PAGE	19. SECURITY CLASSIFICATION OF ABSTRACT	20. LIMITATION OF ABSTRACT

DTIC QUALITY INSPECTED 3

DEVELOPMENT OF ADVANCED ELECTRONIC MATERIALS AND DEVICES FOR ULTRA-LOW 1/F NOISE AND LOW LEAKAGE CURRENT APPLICATIONS

FINAL TECHNICAL REPORT

by

Peter H. Handel

Department of Physics, University of Missouri, St. Louis, MO 63121

July 15, 1997

SUMMARY

The present report contains practical applications of the Quantum 1/f Effect, further development of the Quantum 1/f Theory, and contributions not directly based on quantum 1/f noise. The application to quartz resonators has been improved by the inclusion of crystal defects in the quantum 1/f noise calculation, and has been generalized to the case of low-Q and surface acoustic wave devices, where Q is the quality factor. The generalization is of great practical and theoretical importance, because it introduces the notion of incoherence between the quantum 1/f fluctuations of the phonon loss rate of various regions in the volume of the crystal. The applications also include calculation of quantum 1/f noise in gallium nitride, a material an increased number of uses and with a bright future in microelectronics and opto-electronics. The level of 1/f noise is found to be 3-10 times lower in GaN than in GaAs.

The quantum 1/f theory was reformulated to put in evidence the manifest entropy conservation of the quantum 1/f fluctuation process with the help of the Quantum Information Theory and the notion of negative quantum conditional entropy. This reformulation of the theory on the basis of the new negative entropy concept explains the apparent entropy production with the help of a simultaneous production of negative entropy soft photon states. A long-standing conceptual difficulty is eliminated on this basis.

Of tremendous practical and theoretical importance is the discovery during this grant of a new method of connecting the coherent and conventional quantum 1/f effects. A mass distribution has been found, which allows to find the quantum 1/f noise in general.

Finally, a method of gate current suppression in HFET with high dielectric constant gate insulation and a two-dimensional all-optical time-division multiplexing system were studied.

DEVELOPMENT OF ADVANCED ELECTRONIC MATERIALS AND DEVICES FOR ULTRA-LOW 1/F NOISE AND LOW LEAKAGE CURRENT APPLICATIONS

Contents

I. INTRODUCTION

The present Technical Report contains a brief presentation of the main achievements obtained by the author during the three years of the AFOSR grant F49620-94-1-0342. These achievements are both of practical and of theoretical nature, the close interconnection of these two aspects being a main characteristic of our research.

Our account will start with new *practical* results in the high-tech field, specifically, with a necessary generalization of the author's quantum 1/f theory of frequency fluctuations in the case of ultra-high-Q quartz resonators to the important case of intermediate and low-Q resonators. The first case, generalized in the present grant period to crystals with lattice defects, is essential for the best resonators at NIST, the National Institute of Standards and Technology. They help define the limits of our notion of time and frequency, and we present this case in Sec. II. The second case is the basis of our industrial applications of bulk acoustic wave (BAW) and surface acoustic wave (SAW) quartz resonators. It is given in Sec. III.

New III-V materials such as GaN are of increasing importance for HFETs. GaN has been used to produce semiconductor lasers and LEDs over wide frequency domains, up to the blue region. III-V materials are also used in advanced infrared imaging arrays and in novel piezoelectric III-V semiconductor devices. All these new materials and devices are affected by the conventional and often, if they are larger, also by the coherent quantum 1/f noise effect. During the previous grant period, the conventional quantum 1/f effect was calculated in detail as a function of temperature and doping level for Si and GaAs, as reported in the 1994 Final Report. In order to help in the development of the new technology, as shown in Sec. IV., we have calculated the quantum 1/f noise in GaN, thereby enabling the quantum 1/f optimization process for this material.

Fundamental progress in understanding the nature of the measurement process and in eliminating a basic contradiction of quantum mechanics was recently obtained on the basis of the new Quantum Information-Theoretical Approach. This fundamental progress is based on the new notion of Negative Quantum (von Neumann) Entropy of quantum entangled states. The contradiction between the well-known unitary character of the evolution of the state of a system, which precludes any increase in entropy, and the actual increase of the entropy of the system as a result of the measurement process has been eliminated for the first time.

The present author has applied this fundamentally new concept of negative entropy for the first time to the conventional quantum 1/f effect, as shown in Sec. V. As a result, a way to eliminate the long-standing contradiction of the entropy of quantum 1/f noise appearing from nowhere was found. The entropy of quantum 1/f noise, which was thought to violate the unitarity of the evolution of the combined system of electromagnetic field and charged particles carrying a current, has now been shown by us to be fully compensated by the negative entropy of the entangled electromagnetic bremsstrahlung field. No other known phenomenon was so deeply affected in its understanding by the notion of Negative Quantum Entropy as the Quantum 1/f Effect. The derivation of the conventional quantum 1/f effect and of the Quantum 1/f Entropy, without the use of any assumptions about the non-unitary character measurement process, is presented in Sec. V.

The quantum 1/f theory provides answers for any questions concerning the fundamental 1/f noise, just as Maxwell's equations answer for electromagnetism. Therefore, the quantum 1/f theory must also provide the correlations of any order as well as the joint 1/f noise distributions and momenta of any order for any number of time arguments. This ultimate, exhaustive and total information is contained in the characteristic functional of the process, derived for subtle case of thermal noise in Sec. VI. The characteristic functional for quantum 1/f current noise was derived earlier. Finally, we note that the fractal dimension of a 1-dimensional model of the quantum 1/f effect was derived during the previous grant period, as shown in the 1994 Report, but the general case has not been solved so far due to mathematical complexity.

A long-standing fundamental problem in the quantum 1/f theory is the continuous transition between the coherent and conventional quantum effects for intermediate sizes of the semiconductor or metallic sample or device. The main problem was that in spite of the obvious relation of the two effects as two aspects of the same phenomenon, it was not clear how to improve on the well-

known 1985 interpolation result, or even how to start. A possible practical way of proceeding was developed during this grant and is presented in Sec. VII. This represents a new way of bridging the intermediary region of device sizes.

Other, less fundamental progress, has been achieved during this grant in the following directions: 1) Application of ferroelectric and high ε paramagnetic materials to the design of high-transconductance HFETs with low 1/f noise and low gate leakage current, as demonstrated in Sec. VII; 2) Discovery of a two-dimensional all-optical parallel-to-series TDM and de-multiplexing by spectral-holographic method for radical noise reduction and better channel capacity utilization -- this one is also fundamental, but from a practical point of view, as we see in Sec. VIII; 3) Development of quantum 1/f formulas for efficient FET and HFET Quantum 1/f noise optimization; 4) Development of quantum 1/f formulas for the three independent noise sources in BJTs and HBTs, their integration in master formulas and their use for efficient device optimization; 5) Development of methods for base resistance evaluation from 1/f noise measurements; 6) Quantum 1/f optimization formulas for FET and HFET materials; 7) Quantum 1/f material optimization formulas for junction type devices: junctions, BJTs and HBTs; 8) Quantum 1/f optimization of amplifiers; 9) Quantum 1/f optimization of oscillators; and 10) Quantum 1/f optimization of laser clocks. 11) Discovery of the "thermo-electrochemical effect". These points are discussed briefly below in relation to the corresponding papers mentioned in the list of publications during the grant in Sec. XI:

1. The nature of the transition between the coherent and conventional quantum 1/f formulas has been clarified and described for the first time on the basis of an effective quantum 1/f rest mass distribution of the electron. This allows us to describe in detail how the coherent quantum 1/f contribution is effectively reduced to conventional quantum 1/f noise when the size of a sample is decreased. Refer to papers #7 and 3 in the list of publications during the grant.

2. To provide a service to the scientific community at large, the nature and origin of the excess heat observed even in the "closed cell" variant of electrolytic "cold fusion" experiments has been discovered. The effect can now be calculated with a simple formula, and the "hidden variable" which caused the effect to be absent sometime, was clearly identified. The quantum 1/f philosophy was applied to this case. Like in the quantum 1/f effect, the hidden interaction of the system with the rest of the world turned out to be the origin of this elusive excess heat effect. The new effect discovered in this process was named by the author as the "thermo-electrochemical effect" which will require considerable renormalization of many electrochemical-thermodynamical data and tables. It causes the electrochemical closed system cell to work like a heat pump, even if there is no circulation of electrolyte or coolant (the system being closed, self-contained and ideally insulated). Refer to papers #16 and 2 in the list of publications during the grant. The discovery caused a partial reconciliation of the physics and chemistry communities in the "cold fusion" debate, a reorientation of most "cold fusion" efforts, and a reduction in funding for those involved in this field.

3. The quantum 1/f effect was applied to atomic frequency standards, such as the Cs and Rb clocks, yielding a quantum 1/f flicker floor one or two orders of magnitude below the observed level of fluctuations. This indicates that the quantum limit has not yet been reached in the case of these clocks. A similar situation was found in the case of H-maser clocks, and for the new laser clocks. All of these devices are operating at fluctuation levels well above their quantum 1/f limit. Refer to papers #4, 8, and 10 in the list of publications during the grant.

4. A study of possible approaches to reducing the gate current of HFETs while increasing their transconductance and reducing their noise has shown that high-ε gate insulation provides the best solution. This result was presented at the WOFE workshop (Tenerife, 1997), and has motivated exploratory research into the practicality and optimal realization of this solution. Refer to paper #12 in the list of publications during the grant.

5. A two-dimensional all-optical multiplexing and de-multiplexing scheme has been suggested with the use of spectral-holographic four-wave mixing methods. This system uses a multiple-quantum well device as its nonlinear element. At this point it is not clear whether the aberration, quantum 1/f, hysteresis, and device non-uniformity caused noises can all be held

5

sufficiently low at the MQW device in order to make this suggestion useful. Refer to paper #13 in the list of publications during the grant.

6. The new concept of negative quantum entropy has been successfully applied by the PI to the quantum 1/f effect for the first time in 1996, and presented at the January 1997 WOFE workshop in Tenerife and at the May 1997 Orlando Frequency Control Symposium. The concept had been developed earlier in 1996 and explained why the entropy increases in measurements although quantum mechanical evolution is unitary and precludes entropy increase in pure states. The PI's application of this new quantum information-theoretical concept to the quantum 1/f effect resolves basic questions related to the entropy increase generated by the quantum 1/f effect. Refer to papers #14 and 15 in the list of publications during the grant.

7. Finally, the application of the quantum 1/f theory to high-Q quartz resonators and frequency standards mentioned above in points 2 and 12 above was extended for the first time to the general incoherent case of lower-Q and surface-acoustic-wave quartz resonators. This development, important for practical technical applications and for the optimization of quartz devices and systems was presented at the May 1997 Annual Frequency Control Symposium in Orlando. Refer to paper #15 in the list of publications during the grant.

8. Other progress, so far unpublished, included work on: 1) Quantum 1/f formulas for FET and HFET Quantum 1/f noise optimization; 2) Development of quantum 1/f formulas for the three independent noise sources in BJTs and HBTs; 3) Methods for BJT and HBT base resistance evaluation from 1/f noise measurements; 4) Quantum 1/f optimization formulas for FET and HFET materials; 5) Quantum 1/f material optimization formulas for junction type devices: junctions, BJTs and HBTs; 6) Quantum 1/f optimization of amplifiers; 7) Quantum 1/f optimization of oscillators.

The present state concerning 1/f noise in high-tech applications is still characterized by a serious discrepancy. A new understanding of the fundamental quantum nature of low-frequency (1/f) noise has been achieved, but in practice, most high-technology devices still operate far above the quantum limit defined by the new theory. Actually, the quantum limit can be achieved, and even this limit could be lowered in practice by improving the design on the basis of the quantum 1/f theory.

The trouble is localized both at the level of the materials used and at the level of device design. Other detrimental aspects are the presence of large leakage currents in heterostructure field effect transistors (HFET, studied at the Wright Patterson AFB by F. Schuermeyer) or junction devices (studied at Hanscom Rome AFB by J.M. Mooney and N.F. Yannoni), and the lack of a satisfactory quantum theory of mesoscopic devices which starts from a quantum admittance theory of highly transmissive devices. The former causes very detrimental signal power drain as well as large 1/f noise, while the latter causes device builders to overlook many possibilities offered by quantum interference and tunneling effects in submicron devices.

The quantum 1/f effect is a fundamental fluctuation of all currents of charged particles j, of all scattering cross sections σ_s, recombination cross sections σ_r, tunneling rates or transition rates of any kind Γ, in short of all physical cross sections σ and process rates Γ, given by the universal formula $S(f) = 2\alpha A/fN$ (conventional quantum 1/f equation [1-13]) for small devices, and $= 2\alpha/\pi fN$ (coherent quantum 1/f equation [13-16]) for large devices. These two forms can be combined into a single general formula, as we show below. Here $S(f)$ is the spectral density of fractional fluctuations in current, $\delta j/j$, in scattering or recombination cross section $\delta\sigma/\sigma$, or in any other process rate $\delta\Gamma/\Gamma$. $\alpha = e^2/\hbar c = 1/137$ is Sommerfeld's fine structure constant, a magic number of our world depending only on Planck's constant $\hbar$, the charge of the electron e and the speed of light in vacuum c. $A = 2(\Delta v/c)^2/3\pi$ is essentially the square of the vector velocity change Δv of the scattered particles in the scattering process whose fluctuations we are considering, in units of c. Finally, N is the number of particles used to define the notion of current j, of cross section σ or of process rate Γ.

II. INCOHERENCE OF THE QUANTUM 1/F EFFECT IN LOW-Q BAW AND SAW QUARTZ RESONATORS

1. Introduction

The application of the quantum 1/f theory to bulk acoustic wave (BAW) and surface acoustic wave (SAW) quartz resonators has so far been limited to the case of very high Q resonators in which the phonons are coherent throughout the resonator volume. Here the quantum 1/f theory is applied to the general case of an arbitrary coherence length of the phonons, which may be large or small compared with the size of the quartz resonator. This allows to extend the theory for the first time to low-Q resonators in which the phonons are localized in a part of the resonator volume. The theory is also extended to include defect scattering along with the phonon scattering case exclusively published so far.

Phonon scattering in the resonator is known to limit the short- and medium-term frequency stability in all quartz resonators [17]. Phonon scattering can occur on other phonons (particularly at higher temperatures) or on crystal defects (favored by default at low temperatures). In both cases this process is shown to yield a 1/f spectrum of resonator frequency fluctuations through the conventional Quantum 1/f Effect. As was first shown on this basis with the help of a simple harmonic oscillator model [18], BAW and SAW quartz resonators ought to have a Q^{-4} dependence of their FM power spectrum. This has been experimentally verified by Gagnepain and Uebersfeld for BAW resonators [19] when they first noticed their $1/Q^{4.4}$ law, and by Parker for the SAW case[20]. Although the quantum 1/f effect provided the historical basis for the derivation of the Q^{-4} law [18] as being caused by fluctuations in the dissipation rate of the quartz resonator, the exact mechanism through which the quantum 1/f effect modulates the dissipation rate remained unknown from 1978 to 1991.

Finally, the bridge directly connecting 1/f noise in frequency standards to the quantum 1/f effect was discovered [21]-[23]. Here is how it works. The rate Γ of photon-interactions which remove phonons from the main quartz resonator mode is modulated by the quantum 1/f effect, therefore exhibiting observable quantum fluctuations, while its expectation value remains constant. Indeed, whenever a phonon is removed from the main resonator mode, the time-derivative of the polarization vector of the quartz crystal $dP/dt=\dot{P}$, is suddenly jolted, suffering a step-like modification as a function of time. From Maxwell's equations we know, however, that $\dot{P}$ is added to the current J and that such a modification of the current causes radiation. Solving Maxwell's equations we find that as a result of the phonon removal there is a constant energy of $(1/4\pi\varepsilon_0)4(\Delta\dot{P})^2/3c^3$ radiated away per unit frequency, i.e. per Hertz at any frequency f. Dividing this result by the energy of a photon hf, we find that there is thus a probability of $2\alpha(\Delta\dot{P})^2/3\pi fe^2c^2$ for the emission (radiation) of a bremsstrahlung photon of frequency f. Here $\alpha = (1/4\pi\varepsilon_0)(2\pi e^2/hc) = 1/137$ is Sommerfeld's fine structure constant, a dimensionless universal constant constructed from Planck's constant, the charge e of the electron, and the speed of light c. SI units are used here, while Gaussian units were used in [23].

Since there is a probability of $2\alpha(\Delta\dot{P})^2/3\pi fe^2c^2 \ll 1$ for the emission of a photon of frequency f, the quartz crystal suffers a reaction, or a recoil, in its quantum state, causing the phonon-emission rate Γ to perform quantum oscillations with frequency f and with two-sided spectral density S' of fractional fluctuations given by the same expression, $S'_{\delta\Gamma/\Gamma}(f) = 2\alpha(\Delta\dot{P})^2/3\pi fe^2c^2$. This is the quantum 1/f effect. The one-sided spectrum is thus

7

$$S_{\delta\Gamma/\Gamma}(f) = 4\alpha(\Delta\dot{\mathbf{P}})^2/3\pi f e^2 c^2. \tag{1}$$

This means that any radiation caused or implied by a quantum transition from one state to another comes with a price: it reacts back on the system, causing the rate of that transition to be modulated by exhibiting observable macroscopic quantum fluctuations with a spectral density of fractional rate fluctuations identical to the photon emission probability accompanying the transition considered. No knowledge of quantum mechanics is therefore needed in order to apply the quantum 1/f effect, provided one manages to divide the energy radiated by the energy hf of one photon of frequency f, i.e., provided one accepts just the reality of Planck's constant h and Planck's relation between photon energy and frequency. Knowledge of electrodynamics is needed, however, in order to calculate the energy radiated in a transition.

The reader interested in a basic understanding of the quantum 1/f effect will find a most accessible description at the end of p. 8 and beginning of p. 9 in [24]. That description considers scattering of electrons as an example of transition which emits radiation and suffers a quantum 1/f modulation of its rate, rather than considering scattering of phonons, which, as we believe, is most important in quartz resonators. All that is involved in that derivation is the notion of DeBroglie wave associated to a particle, or the notion of wave function. Pre-quantum mechanics notions are thus sufficient for a basic understanding of the recoil, or energy-loss mechanism, of the quantum 1/f effect (Q1/fE). For a practical application of the Q1/fE, however, classical physics is sufficient.

2. Spatial incoherence of phonon loss rate fluctuations in low and intermediate Q resonators.

The treatment [21]-[23] we have provided so far, assumes that the photons are spread over the whole crystal, and that therefore there is coherence of the quantum 1/f phonon loss rate fluctuations throughout the resonator volume. In the limit of very high Q resonators, and of high resonator frequency, the mean free path and the coherence length ε of the phonons exceed the size of the resonator and our assumption is justified. However, in the low Q and low frequency case the coherence length is small compared with the dimensions of the resonator crystal. The resonator volume is then composed of many incoherent regions of volume ε^3 which fluctuate independently. This is applicable in particular to SAW resonators, as suggested empirically by Parker et al. [25], [26]. We are here borrowing their notation of the size of the coherent volume elements by ε. Considering the $\nu=V/\varepsilon^3$ independently fluctuating regions similar, we replace Eq. (1) by

$$S_{\delta\Gamma/\Gamma}(f) = \sum_{i=1}^{\nu}<(\delta\Gamma_i/\Gamma)^2>_f = \nu^{-1}<(\delta\Gamma_i/\Gamma_i)^2>_f =4\alpha(\Delta\dot{\mathbf{P}}_i)^2/3\pi f\nu e^2 c^2. \tag{2}$$

Here we assumed that $\Gamma=\nu\Gamma_i$ and that $<(\delta\Gamma_i/\Gamma_i)^2>_f = \nu S_{\delta\Gamma/\Gamma}(f)$ is independent of i. With $\nu=V/\varepsilon$ we finally obtain

$$S_{\delta\Gamma/\Gamma}(f) =4\alpha\varepsilon^3(\Delta\dot{\mathbf{P}}_i)^2/3\pi f V e^2 c^2 \tag{3}$$

in the incoherent domain i.e., for sufficiently large V and small Q. The corresponding fluctuations in the frequency ω of the quartz resonator are derived from the equations

$$\omega^2 = \omega_o^2 -2\Gamma^2, \qquad \omega\delta\omega = -2\Gamma\delta\Gamma; \qquad S_{\delta\omega/\omega}(f) = (1/4Q^4)S_{\delta\gamma/\gamma}(f), \tag{4}$$

in which ω_0 would be the natural frequency of the unloaded quartz resonator mode in the absence of the dissipation Γ. Therefore the spectral density of fractional frequency fluctuations $S_{\delta\omega/\omega}(f)$

8

will display the same 1/V dependence in the incoherent regime, down to a volume $V \approx \varepsilon$. Below this volume we expect a proportionality of $S_{\delta\omega/\omega}(f)$ with the volume. Consequently, $S_{\delta\omega/\omega}(f)$ will first increase proportional to 1/V in the incoherent region, and will decrease proportional to V when V is lowered to values below ε. This line of thought, however, neglects the fact that resonators operate usually in the lowest vibration mode, and that therefore a decrease in volume will correspond to a certain increase in the frequency ω_0. The latter is also connected with the speed of the sound c_s and the acoustic attenuation length $l=1/\alpha_{ac}=2c_sQ/\omega_0 \approx \varepsilon$.

The phonon mean free path is about 40 Å for bulk wave phonons in quatz at room temperature and 500 Å at liquid nitrogen temperatures. This approximates the phonon coherence length ε very well. For SAW phonons the corresponding coherence length values may be 4 times lower due to the smaller velocity of the surface wave and due to its stronger scattering.

In a SAW quartz resonator the wave is localized within about two coherence lengths ε from the surface. Therefore, in the incoherent regime $V = 2\varepsilon A$ is a good approximation. Consequently, we expect an increase of $S_{\delta\omega/\omega}(f)$ proportional with 1/A when the resonant area A is decreased, down to very small areas of the order of ε^2.

The incoherence encountered here is similar to the incoherence introduced spatially by the very small coherence length of electrons in semiconductors, of the order of 30Å. The quantum 1/f effect and therefore the measured 1/f noise, has no spatial correlations in semiconductors down to this very small length scale. No other 1/f noise "models" can explain this experimental fact. The quantum 1/f contributions from each electron are independent, which causes a factor $1/N_e$ to be present in all quantum 1/f effect formulas. Here N_e is the number of electrons present in the sample, which had the transition considered as their last interaction.

In the following section we consider the quantum 1/f effect in a resonator volume of size equal or smaller than ε in all directions, the result being applicable whether or not it represents the whole resonator mode.

III. SPATIAL COHERENCE OF THE Q1/f PHONON LOSS RATE FLUCTUATIONS IN HIGH-Q RESONATORS INCLUDING DEFECT SCATTERING.

Let the resonator volume V be smaller than the phonon coherence length ε in all directions. Then $\nu=1$ and we can use Eq. (1). In Eqs. (1)-(3), $(\Delta\dot{P})^2$ is the square of the dipole moment rate change associated with the process causing the removal of a phonon from the main oscillator mode: scattering of a main resonator mode phonon on a themal phonon of higher frequency $\langle\omega\rangle \approx kT/\hbar$. After this, we will include also the case of defect scattering below. To calculate $(\Delta\dot{P})^2$, we write the energy W of the interacting mode $\langle\omega\rangle$ in the form

$$W = n\hbar\langle\omega\rangle = 2(Nm/2)(dx/dt)^2$$

$$=(Nm/e^2)(e\,dx/dt)^2=(m/Ne^2)\varepsilon^2(\dot{P})^2; \tag{5}$$

The factor two includes the potential energy contribution. Here m is the reduced mass of the elementary oscillating dipoles, e their charge, g a polarization constant of the order of the unity, and N their number in the resonator. Applying a variation $\Delta n=1$ we get

$$\Delta n/n = 2|\Delta\dot{P}|/|\dot{P}|, \text{ or } \Delta\dot{P}=\dot{P}/2n. \tag{6}$$

9

Solving Eq. (5) for $\dot{P}$ and substituting into (6), we obtain

$$|\Delta\dot{P}| = (N\hbar<\omega>/n)^{1/2}(e/2g). \tag{7}$$

Substituting $\Delta\dot{P}$ into Eq. (1), we get

$$\Gamma^{-2}S_\Gamma(f) = N\alpha\hbar<\omega>/3n\pi mc^2fg^2 \equiv \Lambda/f . \tag{8}$$

This result is applicable to the fluctuations in the loss rate Γ of the resonator volume.

From Eq. (4) the corresponding resonance frequency fluctuations of the quartz is given for $V\leq\varepsilon$ by

$$\omega^{-2}S_\omega(f) = (1/4Q^4)(\Lambda/f) = N\alpha\hbar<\omega>/12n\pi mc^2fg^2Q^4; \tag{9}$$

where $Q = \omega/2\Gamma$ is the quality factor of the single-mode resonator considered, and $<\omega>$ is not the circular frequency of the main resonator mode, but rather the practically constant frequency of the average interacting (thermal) phonon. Indeed, there are an average $n_\omega=kT/\hbar\omega$ phonons present in any mode of frequency ω. For the case of quartz resonators we have used the interacting thermal mode of average frequency $<\omega>$ to calculate the quantum 1/f effect. The corresponding $\Delta\dot{P}$ in the main resonator mode of frequency ω_0 has to be also included, but is negligible because of the very large number n of phonons present in the main resonator mode and entering in the denominator of Eqs. (7)-(9).

Considering also Eq. (3), Eq. (9) can be written in general with $N\equiv VN/V$ in the form

$$S(f) = \beta'V/fQ^4, \text{ for } V\leq\varepsilon, \tag{10}$$

and

$$S(f) = \beta'\varepsilon^2/fVQ^4, \text{ for } V\geq\varepsilon, \tag{11}$$

where, with an intermediary value $<\omega>=10^8/s$, with $n=kT/\hbar<\omega>$, T=300K and kT=4 $\cdot 10^{-21}$ J

$$\beta' = (N/V)\alpha\hbar<\omega>/12n\pi g^2mc^2$$
$$= 10^{22}(1/137)(10^{-27}10^8)^2/12kT\pi10^{-27} 9\ 10^{20} = 1. \tag{12}$$

For the case of defect scattering, a two-phonon process takes place. A phonon from the main resonator mode scatters on a defect and a phonon of comparable frequency emerges into another mode with much smaller phonon occupation number $n_\omega=kT/\hbar\omega$. In this case we have to replace $<\omega>$ by ω and $n_{<\omega>}$ with n_ω, which gives a β-value which is $(<\omega>/\omega)^2$ smaller, i.e. 10^4-10^6 times smaller. In general, therefore, writing $\Gamma=\Gamma' + \Gamma''$, we obtain for the combined phonon and defect scattering case, in general,

$$\beta=\beta' [\Gamma'^2 + (<\omega>/\omega)^2\Gamma''^2]/\Gamma^2. \tag{13}$$

Although the defect scattering term is small at room temperature, it may become dominant at low

10

temperatures, when the phonon scattering rate Γ' becomes much smaller than the defect scattering rate Γ''.

The form of Eqs. (10)-(13) shows that the level of 1/f frequency noise depends not only as Q^{-4} as previously proposed [18], but also on the oscillation frequency or the volume of the active region. This theory qualitatively fits the data of Gagnepain who varied the Q-factor with temperature in the same quartz resonator (but not frequency or volume), the data of Walls who considered several quartz reonators which differ in volume and frequency, and the data of Parker for SAW resonators, with their relatively low Q values.

The theory also provides the basis for predicting from first principles, without adjustable parameters, how to improve the 1/f level of resonators, beyond just improving the Q-factor, which has been known for many years, and which has been related [18] to fluctuations in the dissipation. Since the 1/f noise level depends on the active volume, in the coherent regime one should use the lowest overtone and smallest diameter consistent with other circuit parameters. In the incoherent (low Q) case, the opposite should be considered.

IV. QUANTUM 1/F NOISE IN GaN SAMPLES

Due to the importance of gallium nitride (GaN) for both the solid-state microelectronics and the opto-electronics of the future, a calculation of the fundamental 1/f noise in this material is of primary importance and is long overdue. We start with (1) a simple evaluation of the conventional quantum 1/f effect in impurity or defect scattering, continue with (2) the calculation of the same effect in acoustic phonon scattering and in (3) the particularly important optical phonon scattering. On this basis we calculate then (4) the resulting conventional quantum 1/f effect. This calculation will be done both for n-type and p-type devices approximately, by neglecting corrections introduced by the energy distribution of the electrons and the author's cross-correlations formula. The errors introduced by this approximation are estimated to be in the 10-20% interval. We then calculate(5) the coherent quantum 1/f effect, and provide on this basis (6) a final result for GaN samples of any size and any nature.

1. Impurity or defect scattering. As briefly mentioned at the end of Sec. I and as derived below in Sec. V, the conventional quantum 1/f effect in a scattering cross section σ or recombination rate Γ is given by

$$S_{\delta\sigma/\sigma}(f) = S_{\delta\Gamma/\Gamma}(f) = 2\alpha A/fN \qquad (14)$$

Here S(f) is the spectral density of fractional fluctuations in current, $\delta j/j$, in scattering or recombination cross section $\delta\sigma/\sigma$, or in any other process rate, $\delta\Gamma/\Gamma$. As mentioned above, $\alpha = e^2/\hbar c = 1/137$ is Sommerfeld's fine structure constant, a basic number of our world depending only on Planck's constant $\hbar$, on the charge of the electron e and on the speed of light in vacuum c. $A = 2(\Delta v/c)^2/3\pi$ is essentially the square of the vector velocity change Δv of the scattered particles in the scattering, recombination or tunneling process whose fluctuations we are considering, in units of c. Finally, N is the number of particles used to define the notion of current j, of cross section σ or of process rate Γ.

For impurity or defect -caused scattering we obtain therefore the quantum 1/f coefficient

$$2\alpha A = (4\alpha/3\pi)(\Delta v/c)^2 = (4\alpha/3\pi)(\Delta p/m_{eff}c)^2 , \qquad (15)$$

which is evaluated assuming a thermal energy 3kT/2 for the motion of the current carriers. Note

11

that $4\alpha/3\pi$ is $3.1 \cdot 10^{-3}$. Thus,

$$2\alpha A = (4\alpha/3\pi)<(\Delta v/c)^2> = (4\alpha/3\pi)(6kT/m_{eff}c^2) = 1.2 \cdot 10^{-9} \, (T/300K)(m_0/m_{eff}) \quad (16)$$

and we obtain for electrons with effective mass $m_{eff}= 0.2m_0$ in n-type GaN

$$2\alpha A^{(e)} = 6 \cdot 10^{-9} \quad (17)$$

and for holes with effective mass $m_{eff}= 0.8m_0$ in p-type GaN

$$2\alpha A^{(h)} = 1.5 \cdot 10^{-9}. \quad (18)$$

For comparison, we note that for n-type GaAs with $m_{eff}=0.068m_0$ we had $2\alpha A_e = 1.8 \cdot 10^{-8}$ and for p-type GaAs with $m_{eff}=0.5m_0$ we had $2\alpha A_h = 2.4 \cdot 10^{-9}$. Here m_0 is the free electron mass.

2. Normal phonon scattering. In this case we put in Eq. (15) $|\Delta p| = \Delta E/s$, where $<\Delta E> \approx kT$ is the energy change of the acoustical phonon in the scattering process and s is the speed of sound. We obtain

$$2\alpha A = (4\alpha/3\pi)(kT/m_{eff}cs)^2 = 3 \cdot 10^{-8} \, (T/300K)^2(m_0/m_{eff})^2. \quad (19)$$

Therefore, for electrons with effective mass $m_{eff}= 0.2m_0$ in n-type GaN

$$2\alpha A^{(e)} = 7.5 \cdot 10^{-7} \quad (20)$$

and for holes with effective mass $m_{eff}= 0.8m_0$ in p-type GaN

$$2\alpha A^{(h)} = 4.7 \cdot 10^{-8}. \quad (21)$$

3. Optical phonon scattering. In this case, the fractional quantum 1/f fluctuation $\delta\Gamma/\Gamma$ of the electron scattering rate Γ on a polar optical phonon of momentum $\hbar q$ and energy $\hbar\omega_q \approx \omega_0$ is described by the quantum 1/f coefficient

$$2\alpha A = (4\alpha/3\pi)<(\hbar q/m_{eff}c)^2> = (4\alpha/3\pi)2<(\hbar k/m_{eff}c)^2>$$
$$= (4\alpha/3\pi)(6kT/m_{eff}c^2) = 1.2 \cdot 10^{-9} \, (T/300K)(m_0/m_{eff}), \quad (22)$$

the same as for impurity or defect scattering, and we obtain as before for electrons with effective mass $m_{eff}= 0.2m_0$ in n-type GaN

$$2\alpha A^{(e)} = 6 \cdot 10^{-9} \quad (23)$$

and for holes with effective mass $m_{eff}= 0.8m_0$ in p-type GaN

$$2\alpha A^{(h)} = 1.5 \cdot 10^{-9}. \quad (24)$$

For comparison, we note that for n-type GaAs with $m_{eff}=0.068m_0$ we had $2\alpha A^{(e)} = 1.8 \cdot 10^{-8}$ and for p-type GaAs with $m_{eff}=0.5m_0$ we had $2\alpha A^{(h)} = 2.4 \cdot 10^{-9}$.

<u>4. Resulting conventional quantum 1/f coefficient and spectral density.</u> Both for electrons and holes, the resulting quantum 1/f coefficient of fluctuations in the mobility μ is given by the relation

$$2\alpha A^{(e,h)} = \Sigma_i (\mu/\mu_i)^2 \, 2\alpha A_i^{(e,h)}, \tag{25}$$

where $2\alpha A_i$ is the quantum 1/f coefficient calculated for the scattering process #i which contributes to limiting the observed mobility according to the relation

$$1/\mu = \Sigma_i (1/\mu_i). \tag{26}$$

Finally, if both electrons and holes contribute to the conductivity $\lambda = e(p\mu_h + n\mu_e)$, the spectral density of conventional quantum 1/f fractional fluctuations in λ is

$$S_{\delta\lambda/\lambda}(f) = 2(e^2\alpha/ \, f\lambda^2)[(p\mu_h)^2 A^{(h)}/N_h + (n\mu_e)^2 A^{(e)}/N_e]. \tag{27}$$

This allows for the calculation of quantum 1/f noise in any small sample. The transition to the coherent quantum 1/f effect applicable for large samples is discussed at the end of the next Sec. V.

Our general conclusion is encouraging, and can only help to brighten the future for GaN even more. Specifically, as we have seen above, the conclusion is that small GaN samples and devices offer lower 1/f noise levels than comparable GaAs samples or devices, by a factor of 3 to 10, mainly due to the larger effective masses of the current carriers.

V. NEGATIVE ENTROPY IN THE QUANTUM 1/f EFFECT

1. Schematic derivation of the conventional quantum 1/f effect

The author's recent application of the new Quantum Information Theory Approach (QIT, developed 1996) to Infra Quantum Physics (IQP) explains for the first time the apparent lack of unitarity caused by the entropy increase in the Quantum 1/f Effect (Q1/fE, developed by us 1974). Indeed, he now offers a more rigorous proof of the conventional quantum 1/f effect in this report, which shows that actually there is no resultant entropy increase and therefore unitarity is not violated. His new proof involves the concept of von Neumann Quantum Entropy, including the negative conditional entropy concept for quantum entangled states. The Q1/fE was applied to many high-tech systems, in particular to ultra-small electronic devices. The present report explains how the additional entropy implied by the Q1/fE arises in spite of the entropy-conserving evolution of the system.

The conventional quantum 1/f effect is a fundamental fluctuation of all currents of charged particles j, of all scattering cross sections σ_s, recombination cross sections σ_r, tunneling rates or transition rates of any kind Γ, in short of all physical cross sections σ and process rates Γ, given by the universal formula

$$S(f) = 2\alpha A/fN \tag{28}$$

We present here only a schematic derivation. Let's simplify our world and assume only one electromagnetic mode of the universe would be present, with frequency ω and wave vector k. Consider the field mode in its ground state and a pair of 2 incoming identical charged particles with

the same well-defined wave vector being scattered by some potential. Both the initial and the final state represent a pure state. The initial state is $|++->_0$, where we reserved the first two arguments of the ket for the two electrons and the last (-) for the field. Due to the interaction with the field, the final state will be

$$|f> = (|++-> + \gamma|+-+>/\sqrt{2} + \gamma|-++>/\sqrt{2})/(\sqrt{1+\gamma^2}), \qquad (29)$$

where γ is the emission amplitude of a bremsstrahlung photon, i.e., for the excitation of the field oscillator from its ground state (-) to its first excited state (+). The first two arguments label the state of the charged particles, indicating the presence of an energy loss with (-) and the persistence in the same energy state with (+). The third argument of the kets always labels the field oscillator, as mentioned.

The corresponding density operator of the pure state obtained is $\rho = |f><f|$. Its quantum von Neumann entropy $S/k = \sigma = -Tr(\rho \log \rho)$ is zero.

2. Paradoxical entropy increase in 1/f noise and quantum information theory

Ignoring the field oscillator, i.e., taking the trace of over the field oscillator label, we obtain a classically correlated system, a mixture of 2 pure states, described by the density operator

$$[|++><++| + \gamma^2(|+-> + |-+>)(<+-| + <-+|)/2]/(1+\gamma^2). \qquad (30)$$

The second term gives the Q1/fE at $f=\omega/2\pi$, as we show below. The corresponding entropy is

$$\log(1+\gamma^2) - (\gamma^2\log\gamma^2)/(1+\gamma^2) > 0 \text{ for } 0\leq\gamma^2\leq1. \qquad (31)$$

The entropy of the system thus appears to have increased although according to quantum mechanics it can not increase. Indeed, according to quantum mechanics, time evolution of a state occurs through a unitary transformation. The latter, however, is known to leave $\sigma = -Tr(\rho \log \rho)$ invariant.

The quantum information theory (QIT) solves this paradox. When two systems A and B with quantum von Neumann entropy $\sigma(A) = -Tr_A(\rho_A\log\rho_A)$ and $\sigma(B) = -Tr_B(\rho_B\log\rho_B)$ form a composite system AB of entropy $\sigma(AB) = -Tr_{AB}(\rho_{AB}\log\rho_{AB})$ we can prove that we have to write

$$\sigma(AB) = \sigma(A) + \sigma(B|A) = \sigma(B) + \sigma(A|B), \qquad (32)$$

in perfect analogy with classical entropies or information. We have introduced $\sigma(A|B)$ as the von Neumann entropy of A conditional on B, or the entropy of A when we know B:

$$\sigma(A|B) = -Tr_{AB}[\rho_{AB}\log\rho_{A|B}]. \qquad (33)$$

Here we have introduced the conditional density matrix $\rho_{A|B} = \rho_{AB}(1_A\otimes\rho_B)^{-1}$, the quantum analog similar to the classical conditional probability, where $\otimes$ is the tensor product in the joint Hilbert space and $\rho_B=Tr_A(\rho_{AB})$ is the marginal density matrix obtained by taking a partial trace over the variables associated with A.

3. Negative entropy and solution of the paradox

The conditional entropy is usually negative in quantum entangled states. Finally, we

14

introduce the quantum mutual entropy which represents the shared entropy, corresponding to the mutual information between A and B:

$$\sigma(A:B) = -Tr[\rho_{AB}\log\rho_{A:B}] \equiv \sigma(A) + \sigma(B) - \sigma(AB), \tag{34}$$

where

$$\rho_{A:B} = \rho_{AB}(\rho_A \otimes \rho_B)^{-1}. \tag{35}$$

Taking all logarithms in the base of 2, the entropies will be expressed in bites. Considering our paradoxical case discussed above for simplicity with $\gamma^2=1$, we obtain the following entropy diagram of our quantum mechanically entangled triplet of three systems comprising the charged particles A and B, as well as the field oscillator C:
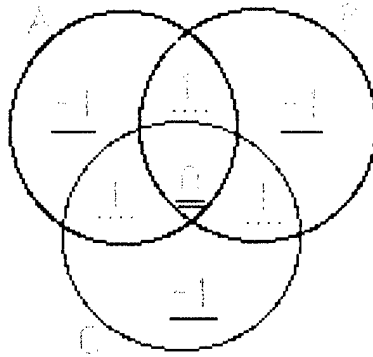

Fig. 1.

Here the quantum conditional entropies are underlined for emphasis, and the mutual quantum entropy has double underlining. Dotted underlining marks the mutual entropy of two of the subsystems, which is, however, not the mutual entropy of the whole system. We see that A, B and C have each 1 bit of entropy, as we expect, since each can be in a + or - state. In addition, $\sigma_{ABC} = 0$ as expected for a pure state. The negative conditional entropies indicate that this state is a pure quantum state which can not be obtained in classical physics.

    If we ignore C by tracing over it, we obtain the classically correlated system AB with its positive entropy of 1 and the negative quantum entropy state of the ignored field oscillator, conditional on AB:
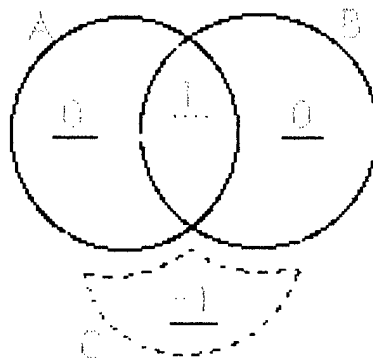

Fig. 2.

    In conclusion, the negative conditional entropy of the ignored field oscillator compensates the positive entropy of the system of two particles. Unitarity and entropy conservation are both satisfied. This is the solution of the paradox. It explains why our earlier explanation of the Q1/fE in terms of a two-particle wave function was correct, in spite of the

15

apparent lack of unitarity.

4. Derivation of the conventional quantum 1/f effect

In the rest of the present section we apply the scheme developed here to the real world with all field oscillators present in $|++\to_o$ and with N incident particles in $|++\to_o$.

We start with the expression of the Heisenberg representation state $|f>$ of N identical bosons of mass M emerging at an angle θ from some scattering process with undetermined bremsstrahlung energy losses reflected in their one-particle waves $\varphi_i(\xi_i)$

$$|f> = (N!)^{-1/2} \Pi_i \int d^3\xi_i \varphi_i(\xi_i)\psi^+(\xi_i) \, |0> = \Pi_i \int d^3\xi_i \varphi_i(\xi_i) \, |f^o>, \qquad (36)$$

where $\psi^+(\xi_i)$ is the field operator creating a boson with position vector ξ_i and $|0>$ is the vacuum state, while $|f^o>$ is the vacuum field state with N bosons of position vectors ξ_i with i = 1...N. All products and sums in this section run from 1 to N, unless otherwise stated.

To calculate the particle density autocorrelation function in the outgoing scattered wave, we need the expectation value of the operator

$$O(x_1,x_2) = \psi^+(x_1)\psi^+(x_2)\psi(x_2)\psi(x_1), \qquad (37)$$

known as the operator of the pair correlation. Using the commutation properties of the boson field operators, we first calculate the matrix element

$$N!<S^o|O|f^o>=$$
$$\Sigma'_{\mu\nu}\Sigma'_{mn}\delta(\eta_\nu-x_1)\delta(\eta_\mu-x_2)\delta(\xi_n-x_1)\delta(\xi_m-x_2)\Sigma_{(i,j)}\Pi'_{ij}\delta(\eta_j-\xi_i). \qquad (38)$$

Here the prime excludes $\mu=\nu$ and m=n in the summations and excludes i=m, i=n, j=μ and j=ν in the product. The summation $\Sigma_{(i,j)}$ runs over all permutations of the remaining N-2 values of i and j. On this basis we now calculate the complete matrix element

$$<f|O|f> = [1/N(N-1)] \Sigma'_{\mu\nu}\Sigma'_{mn}\int d^3\eta_\mu\int d^3\eta_\nu\int d^3\xi_m\int d^3\xi_n$$
$$\varphi_\mu^*(\eta_\mu)\varphi_\nu^*(\eta_\nu)\varphi_m(\xi_m)\varphi_n(\xi_n)\delta(\eta_\nu-x_1)\delta(\eta_\mu-x_2)\delta(\xi_n-x_1)\delta(\xi_m-x_2). \qquad (39)$$
$$= [1/N(N-1)] \Sigma'_{\mu\nu}\Sigma'_{mn} \varphi_\mu^*(x_2)\varphi_\nu^*(x_1)\varphi_m(x_1)\varphi_n(x_2)$$

The one-particle states are spherical waves emerging from the scattering center located at x=0:

$$\varphi(x) = (C/x)e^{iKx} [1 + \Sigma_{kl}b(k,l)e^{-iqx} a^+_{k,l}]. \qquad (40)$$

Here C is an amplitude factor, K the boson wave vector magnitude, γ = b(k,l) the bremsstrahlung amplitude for photons of wave vector **k** and polarization l, while $a^+_{k,l}$ is the corresponding photon creation operator, allowing the photon state to be created from the vacuum if Eq. (40) is inserted into Eq. (36). The momentum magnitude loss q=Mck/hK=Mf/hK is necessary for energy conservation in the Bremsstrahlung process. Substituting Eq. (10) into Eq. (9), we obtain

$$<f|O|f> = |C/x|^4\{N(N-1) + 2(N-1)\Sigma_{k,l}|b(k,l)|^2[1+\cos q(x_1-x_2)]\}, \qquad (41)$$

where we neglected a small term of higher order in b(k,l). To perform the angular part of the summation in Eq. (41), we calculate the current expectation value of the state in Eq. (40), and compare it to the well known cross section without and with bremsstrahlung

$$\mathbf{j} = (h\mathbf{K}/Mx^2)[1 + \Sigma_{kl}|b(k,l)|^2] = \mathbf{j}_o[1 + \int\alpha A df/f], \qquad (42)$$

16

where the quantum fluctuations have disappeared, where $\alpha=e^2/\hbar c$ is the fine structure constant, $\alpha A=(2\alpha/3\pi)(\Delta v/c)^2$ is the fractional bremsstrahlung rate coefficient, also known in QED as the infrared exponent, and the 1/f dependence of the bremsstrahlung part displays the well-known infrared catastrophe, i.e., the emission of a logarithmically divergent number of photons in the low frequency limit. Here Δv is the velocity change $h(K-K_0)/M$ of the scattered boson, and $f=ck/2\pi$ the photon frequency. Eq. (41) gives

$$<f|O|f> = |C/x|^4\{N(N-1) + 2(N-1)(\int\alpha A df/f)[1+\cos q(x_1-x_2)]\}, \qquad (43)$$

which is the pair correlation function, or density autocorrelation function along the scattered beam with df/f=dq/q. The spatial distribution fluctuations along the scattered beam will also be observed as fluctuations in time at the detector, at any frequency f. According to the Wiener-Khintchine theorem, we obtain the spectral density of fractional scattered particle density ρ, (or current j, or cross section σ) fluctuations in frequency f or wave number q by dividing the coefficient of the cosine by the constant term N(N-1):

$$\rho^{-2}S_\rho(f) = j^{-2}S_j(f) = \sigma^{-2}S_\sigma(f) = 2\alpha A/fN \quad [\text{or} =2\alpha A/f(N-1)\text{ for fermions}], \qquad (44)$$

where N is the number of particles or current carriers used to define the current j whose fluctuations we are studying. Quantum 1/f noise is thus a fundamental 1/N effect.

The exact value of the exponent of f in Eq. (44) can be determined by including the contributions from all real and virtual multiphoton processes of any order, and turns out to be αA-1, rather than -1, which is important only philosophically, since $\alpha A\ll 1$. The spectral integral is thus convergent at f=0.

For fermions we repeat the calculation replacing in the derivation of Eq. (38) the commutators of field operators by anticommutators, which finally yields in the same way

$$\rho^{-2}S_\rho(f) = j^{-2}S_j(f) = \sigma^{-2}S_\sigma(f) = 2\alpha A/f(N-1), \qquad (45)$$

which causes no difficulties, since N≥2 for particle correlations to be defined, and which is practically the same as Eq. (44), since usually N≫1. Eqs. (44) and (45) suggest a new notion of physical cross sections and process rates which contain 1/f noise, and express a fundamental law of physics, important in most high-tech applications.

5. Derivation of the coherent quantum 1/f effect

The present derivation is based on the well-known propagator $G_s(x'-x)$ derived relativistically [27-31] in a new QED picture required by the infinite range of the Coulomb potential. The corresponding nonrelativistic form was provided by Zhang and Handel [32]:

$$-i<\Phi_0|T\psi_{s'}(x')\psi_s^\dagger(x)|\Phi_0> \equiv \delta_{ss'}\ G_s(x'-x)$$

$$= (i/V)\sum_p\{\exp i[p(r-r')-p^2(t-t')/2m]/\hbar\}n_{p,s}$$

$$\times\{-ip(r-r')/\hbar+i(m^2c^2+p^2)^{1/2}(t-t')(c/\hbar)\}^{\alpha/\pi}. \qquad (46)$$

Here α is again Sommerfeld's fine structure constant, $n_{p,s}$ the number of electrons in the state of momentum p and spin s, m the rest mass of the fermions, $\delta_{ss'}$ the Kronecker symbol, c the speed of light, x=(r,t) any space-time point and V the volume of a normalization box. T is the time-

ordering operator which orders the operators in the order of decreasing times from left to right and multiplies the result by $(-1)^P$, where P is the parity of the permutation required to achieve this order. For equal times, T normal-orders the operators, i.e., for t=t' the left-hand side of Eq. (46) is $i<\Phi_o|\psi_s^\dagger(x)\psi_{s'}(x')|\Phi_o>$. The state Φ_o of the N electrons is described by a Slater determinant of single-particle orbitals. Eq. (46) is exact at large t-t', or low frequency.

To calculate the current autocorrelation function we need the density correlation function, which is also known as the two-particle correlation function. The two-particle correlation function is defined by

$$<\Phi_o|T\psi_s^\dagger(x)\psi_s(x)\psi_{s'}^\dagger(x')\psi_{s'}(x')|\Phi_o> = <\Phi_o|\psi_s^\dagger(x)\psi_s(x)|\Phi_o><\Phi_o|\psi_{s'}^\dagger(x')\psi_{s'}(x')|\Phi_o>$$

$$- <\Phi_o|T\psi_{s'}(x')\psi_s^\dagger(x)|\Phi_o><\Phi_o|T\psi_s(x)\psi_{s'}^\dagger(x')|\Phi_o>. \qquad (47)$$

The first term can be expressed in terms of the particle density of spin s, $n/2 = N/2V = <\Phi_o|\psi_s^\dagger(x)\psi_s(x)|\Phi_o>$, while the second term can be expressed in terms of the Green function (22) in the form

$$A_{ss'}(x-x') \equiv <\Phi_o|\psi_s^\dagger(x)\psi_{s'}^\dagger(x')\psi_{s'}(x')\psi_s(x)|\Phi_o> = (n/2)^2 + \delta_{ss'} G_s(x'-x)G_s(x-x'). \qquad (48)$$

The "relative" autocorrelation function A(x-x') describing the normalized pair correlation independent of spin is obtained by dividing by n^2 and summing over s and s'

$$A(x-x') = 1 - (1/n^2)\sum_s G_s(x-x')G_s(x'-x)$$

$$= 1 - (1/N^2)\sum_s \sum_{pp'}\{\exp i[(p-p')(r-r')-(E_p-E_{p'})(t-t')]/\hbar\}n_{p,s}n_{p',s}$$

$$\times \{p(r-r')/\hbar-(m^2c^2+p^2)^{1/2}(t-t')(c/\hbar)\}^{\alpha/\pi}$$

$$\times \{p'(r'-r)/\hbar-(m^2c^2+p'^2)^{1/2}(t'-t)(c/\hbar)\}^{\alpha/\pi}. \qquad (49)$$

Here we have used Eq. (46). We now consider a beam of charged fermions, e.g., electrons, represented in momentum space by a sphere of radius p_F, centered on the momentum $\mathbf{p_0}$ which is the average momentum of the fermions. The energy and momentum differences between terms of different $\mathbf{p}$ are large, leading to rapid oscillations in space and time which contain only high-frequency quantum fluctuations. The low-frequency and low-wavenumber part A_l of this relative density autocorrelation function is given by the terms with $\mathbf{p} = \mathbf{p'}$

$$A_l(x-x') = 1 - (1/N^2)\sum_s \sum_p n_{p,s}$$

$$\times |p(r-r')/\hbar-(m^2c^2+p^2)^{1/2}(t-t')(c/\hbar)|^{2\alpha/\pi} \qquad (50)$$

$$\approx 1 - (1/N)|p_0(r-r')/\hbar-mc^2\tau/\hbar|^{2\alpha/\pi} \quad \text{for } p_F<<|p_{o3}-mc^2\tau/z|. \qquad (51)$$

Here we have used the mean value theorem, considering the $2\alpha/\pi$ power as a slowly varying function of $\mathbf{p}$ and neglecting $\mathbf{p_0}$ in the coefficient of $\tau \equiv$ t-t', with $z \equiv |r-r'|$. The correlations propagate along the beam with a group velocity given by the average velocity $\mathbf{p_0}/m$ of the particles in the beam, and with the phase velocity of c^2/v. Denoting $\theta \equiv |\tau - \mathbf{p_0}(r-r')/mc^2|$, and using a well known identity for the last step [32], we obtain from Eq. (51) the form

$$A_l(x-x') = 1 - (1/N)|mc^2\theta/\hbar|^{2\alpha/\pi} = 1 -(1.25/N)|\Theta|^{2\alpha/\pi} = 1 -(1.25/N)e^{(2\alpha/\pi)\ln\Theta}$$

$$\approx 1-(1.25/N)[1+(2\alpha/\pi)\ln\Theta] = 1 - (2.5/N) + (1.25/N)[1-(2\alpha/\pi)\ln\Theta] \qquad (52)$$

$$\approx (N-2.5)/N +(1.25/N)e^{-(2\alpha/\pi)\ln\Theta} = (1/N)\{N-2.5+(2.5\alpha/\pi\cos\alpha)\int_0^\infty \cos\omega\Theta d\omega/\omega^{1-2\alpha/\pi}\}.$$

This indicates a $\omega^{-1+2\alpha/\pi}$ or $1/f$ spectrum and a $1/(N-2.5)$ dependence of the spectrum of fractional fluctuations in density n and current j. The total error corresponding to the two linear approximations of exponentials in Eq. (52) is less than 1%, provided $|\ln\Theta|<20$, or $(250,000)^{-1}$ hours $< |\theta| < 250,000$ hours. Here $\Theta=\theta/1s$ and ω is the circular Fourier frequency in rad/s. We have used $[1s\ mc^2/\hbar)]^{2\alpha/\pi} \approx 1.25$; this accounts also for the presence of the number 2.5 instead of the more normal number 2 in the final form. The form we have chosen here is more convenient for applications. The equivalent normal form would have been

$$A_1(x-x') \approx (1/N)\{N-2+(2\alpha/\pi\cos\alpha)\int_0^\infty [mc^2/\hbar\omega]^{2\alpha/\pi}\cos\omega\theta\ d\omega/\omega\}, \qquad (53)$$

in which the error caused by the two linear approximations of exponentials would have been of the order of 20%, and in which the fractional power would also have been neglected in the integrand for all purposes except for the theoretical question of the integrability of the $1/\omega$ spectrum. The fractional autocorrelation of current fluctuations δj is obtained by multiplying Eqs. (52-53) on both sides with $(ep_o/m)^2$, and dividing by $(enp_o/m)^2$ which is the square of the average current density j, instead of just dividing by n^2. So it is the same as the fractional autocorrelation for quantum density fluctuations. The last form of Eq. (52) for the universal coherent quantum-electrodynamical chaos process in electric currents finally becomes

$$S_{\delta j/j}(\omega) \approx [2.5\alpha/\pi\omega(N-2.5)][\omega]^{2\alpha/\pi} \approx 2.5\alpha/\pi\omega N = 0.0058/\omega N. \qquad (54)$$

The spectral density resulting from Eq. (53) coincides with the result $2\alpha/\pi f N$, derived directly earlier [14] from the coherent state of the electromagnetic field of a physical charged particle. The connection with the conventional quantum $1/f$ effect was discussed in Sec. II.1.

Being observed in condensed matter in the presence of a constant applied field, these fundamental quantum current fluctuations are usually interpreted as mobility fluctuations. Most of the conventional quantum $1/f$ fluctuations in physical cross sections and process rates are also mobility fluctuations, but some are also in the recombination speed or tunneling rate.

6. Discussion and conclusions

Consider now the physical basis of the connection with the conventional quantum $1/f$ effect. The energy of the collective (drift) motion of the current carriers has a magnetical component, which we consider coherent, because the field contributions of the individual current carriers are additive

$$E_m = \int(B^2/8\pi)d^3x = [nevS/c]^2\ln(R/r). \qquad (55)$$

Here n is the concentration of current carriers, v their drift velocity, c the speed of light, r the radius and S the area of the cross section of the cylindrical conductor or semiconductor sample considered. There is, however, also a kinetic energy contribution, which is incoherent, because the kinetic energies of the drift motion of the current carriers must be added to get the total kinetic

19

energy, rather than their momenta.

$$E_k = \Sigma mv^2/2 = nSmv^2/2 = E_m/s. \tag{56}$$

The "coherece ratio"

$$s = E_m/E_k = 2ne^2S/mc^2\ln(R/r) \approx 2e^2N'/mc^2, \tag{57}$$

has been introduced here for convenience, where $N' = nS$ is the number of carriers per unit length of the sample and the natural logarithm $\ln(R/r)$ has been approximated by one in the last form. We expect the observed spectral density of the mobility fluctuations to be given by a relation of the form

$$(1/\mu^2)S_\mu(f) = [1/(1+s)][2\alpha A/fN] + [s/(1+s)][2\alpha/\pi fN] \tag{58}$$

which can be interpreted as an expression of the effective Hooge constant if the number N of carriers in the (homogeneous) sample is brought to the numerator of the left hand side

$$\alpha_H = [1/(1+s)]\alpha_{Hconv} + [s/(1+s)]\alpha_{Hcoh}. \tag{59}$$

In this equation $\alpha A = 2\alpha(\Delta v/c)^2/3\pi$ is the usual nonrelativistic expression of the infrared exponent, present in the familiar form of the conventional quantum 1/f effect. This equation is limited to quantum 1/f mobility (or diffusion) fluctuations, and does not include the quantum 1/f noise in the surface and bulk recombination cross sections, in the surface and bulk trapping centers, in tunneling and injection processes, in emission or in transitions between two solids.

Note that the coherence ratio s introduced here equals the unity for the critical value $N' = N'' = 2 \cdot 10^{12}$/cm., e.g. for a cross section $S = 2 \cdot 10^{-4}$ cm^2 of the sample when $n = 10^{16}$. For small samples with $N' \ll N''$ only the first term survives, while for $N' > N''$ the second term in Eq. (59) is dominant.

The conventional and coherent Q1/fE was successfully applied FETs, HFETs, BJTs, and HBTs, as well as to quartz resonators and amplifiers. In conclusion:

-- The quantum 1/f effect appears to generate entropy, but this is only because we do not observe the negative conditional entropy contribution of the emitted soft photons.

-- The quantum 1/f effect contains Planck's constant in the denominator and diverges in the classical limit.

-- The quantum 1/f effect represents a new aspect of quantum physics.

-- The quantum 1/f effect is a form of quantum chaos, arising only from spontaneous bremsstrahlung.

-- The quantum /f effect limits most high-technology applications and devices. Its knowledge allows us to optimize them.

VI. CHARACTERISTIC FUNCTIONAL OF PHYSICAL THERMAL NOISE
- WHICH INCLUDES EQUILIBRIUM QUANTUM 1/f NOISE -

1. Introduction

In a previous paper [33] the characteristic functional of quantum 1/f noise was derived. This result was applicable to quantum 1/f noise in any cross section or process rate, and in currents or voltages. In another paper [34] the application of quantum 1/f noise to thermal equilibrium

noise was performed, and the quantum 1/f Nyquist theorem was formulated. Deviations from the Gaussian form of thermal noise were expressed [34],[35] in terms of the characteristic function.

The Quantum 1/f Effect (Q1/fE) is a fundamental fluctuation phenomenon present as coherent Q1/f Noise $2\alpha/\pi fN$ in electrical currents of any nature and present as conventional Q1/f Noise $2\alpha A/fN$ in the *physical cross sections and process rates* (PCS&PR). The PCS&PR are defined as the scattered current, or the outgoing current resulting from a process, including its quantum fluctuations acquired due to the interaction with the electromagnetic field, all referred to the unit of incoming flux, which is one particle per second per cm^2. The usual notion of cross section or process rate is a quantum-mechanical expectation value which does not contain the quantum fluctuations. In the present report the nature of the quantum 1/f fluctuations introduced by us in 1975 is investigated and described as a form of quantum chaos.

Both Coherent and Conventional Quantum 1/f Noise are peculiar quantum effects. They contain Planck's constant only in the denominator, as part of the fine structure constant to which both are proportional. This implies that they increase without upper bound when we approach the classical limit by letting ħ go to zero. One is left with the impression that the classical limit of the quantum 1/f effects does not exist.

At this point it is useful to remember that the quantum 1/f approach originated from the classical homogeneous and isotropic turbulence theory in an unbounded plasma of electrons and holes [36], [37], and was introduced as the result of prolonged quantization efforts applied to this classical theory. The classical theory corresponded to infinite noise power in any finite frequency interval. Therefore, if we accept quantum 1/f noise as the quantum manifestation of classical turbulence, its infinite classical limit no longer confronts us with conceptual difficulties. Moreover, the physical nature of quantum 1/f noise becomes connected directly to the nature of classical turbulence which is in practice caused by the instability of laminar flow when a certain critical value of the Reynolds number is surpassed.

Being governed by the Navier-Stokes equations, classical turbulence, naturally obtained from the instability of laminar flows, is in fact deterministic, in spite of its stochastic appearance. Therefore we use the word "chaos" to describe its true nature. The transition from laminar flow to turbulence is one of the seven known routes to chaos, the oldest known route in fact. The chaotic nature of turbulence characterizes turbulence as a deterministic process if finite dimensionality dependent on the bandwidth of the turbulent frequencies observed. In the same way, quantum 1/f noise, being governed by the Schrödinger Equation for the chaotic wave fields, is in fact deterministic; it represents the oldest known form of quantum chaos. The finite dimension of quantum 1/f noise was calculated [38] on the basis of a 1-dimensional model of the quantum 1/f theory.

In conclusion, quantum chaos is defined here as the quantum manifestation of classical chaos. The latter, in turn, is defined as the quasistationary state eventually reached by a system after instabilities of the laminar state have triggered the transition into another state characterized by time-dependent values of the dynamical parameters, with a probability distribution law which is stable in time. Our notion of quantum chaos is visualized by the deterministic evolution of the seemingly stochastic Schrödinger field.

As we know, however, the wave function is not directly observable, but rather is a means of calculating the expectation values of observable quantities. Even if the wave function is well defined, due to its probabilistic interpretation, we obtain random, or stochastic fluctuations of the local physical parameters of the system, superposed on the deterministic-chaotic background. We will consider this stochastic component irrelevant for the following reason: the stochastic element enters only because we ask for properties which the system does not have, i.e., because we asked a meaningless question. In quantum mechanics such meaningless questions can be made artificially meaningful by imposing the corresponding properties on the system from outside in the measurement process. This does not mean the system had this property all along, it had instead other, complementary, parameters which were better defined before, but lost their definition in the measuring process. The physical meaning of the superposed stochastic component is that it represents the shot noise, which is well known, given by the spectral density of $2eI$, and which is

21

not the object of our studies. It is worth mentioning, however, that it is a organical component of the noise process which has a deterministic (chaotic), as well as a superposed stochastic component.

The Q1/fE is caused by the infinite range of the electromagnetic interaction, i.e., of the Coulomb field. Any charged particle is thus always in interaction with all other arbitrarily distant charges, and this causes the particle to have an energy, which is not well defined, i.e., a mass, and therefore a relativistic mass shell, which is not sharp. Mathematically, this energy uncertainty is expressed by the fact that the charged particle consists of the bare particle plus its electromagnetic field which in the rest system is just the Coulomb field. The latter is characterized by a well-defined electric field and vector potential. A Fourier transformation then tells us that the electromagnetic field oscillators for any wave vector k and polarization λ have a well defined phase, and are therefore in coherent states. The latter, in turn, are states of indefinite energy, first introduced by Schrödinger in the early days of quantum mechanics, and later used by Glauber to describe coherent states of the electromagnetic field.

How can we express mathematically the stochastic fluctuations and their deterministic-chaotic background? Heisenberg's equations of motion for the density matrix of the system of charged particles whose quantum 1/f current fluctuations are under consideration and of the electromagnetic field modes coupled to them provide the desired description. The solution should be given by the characteristic functional of the current fluctuations. The characteristic functional of conventional quantum 1/f noise $j(t) = J(t) - \langle J \rangle$ affecting the current $I = \langle J \rangle$ has been shown [6] to be

$$H[x(\epsilon)] = \exp[-\alpha A(I^2/N)\int(\epsilon/\epsilon_o)^{\alpha A}|x(\epsilon)|^2 d\epsilon/\epsilon]. \tag{60}$$

Here αA is the infrared exponent $\alpha A = (4\alpha/3\pi) \langle(\Delta v/c)^2\rangle$, which is known to enter the expression of both the basic quantum 1/f noise formula and the characteristic functional of quantum 1/f noise in two ways: as a coefficient and as an additional exponent of the frequency f. Sommerfeld's fine structure constant $\alpha = e^2/\hbar c = 1/137$ is well known, and so is the Boltzmann constant k_B. Eq. (60) gives the characteristic functional of 1/f noise for a sample containing N scattered current carriers with a velocity change $\langle(\Delta v)^2\rangle$ caused the scattering process. Eq. (60) also approximates the characteristic functional of 1/f noise from a solid-state sample containing N current carriers with an average velocity change $\langle(\Delta v)^2\rangle$ in the scattering processes which determine their mobility.

The present report performs the final step in the study of thermal noise with infrared radiative corrections, by calculating the characteristic functional of physical thermal noise. We call it "physical" because we refer to the actually observed thermal equilibrium (Johnson) noise, rather than to the strictly Gaussian noise expected from the Nyquist formula without infrared radiative corrections. The small quantum 1/f contributions come in as time-dependent infrared radiative corrections, required by the interaction of the current carriers with the electromagnetic field, or by the reaction of the bremsstrahlung back on the current which has produced it. Knowing the characteristic functional of a process is the best we can do, the highest level and most comprehensive and complete description possible for a random process.

2. Amplitude Distribution and Characteristic Function

In terms of current fluctuations in equilibrium, to derive the characteristic function of the physical thermal noise current variable ξ, we express it in terms of the unmodulated theoretical Nyquist noise current variable x:

$$\xi = x(G/G_o)^{1/2} = x + xy, \tag{61}$$

where $y = \delta G/2G_o$ is the fractional quantum 1/f fluctuation in the conductivity $G = G_o + \delta G$ of the conductor whose thermal equilibrium current fluctuations we are considering. Let the quantum 1/f

22

noise variable y obey a Gaussian amplitude distribution of dispersion σ_2, and x one of dispersion σ_1. We prove now that in terms of the zero-order Bessel function of imaginary argument, the product $z=xy$ will have an amplitude distribution $P(z)=(1/\pi\sigma_1\sigma_2)K_0(z/\sigma_1\sigma_2)$ which has an elementary characteristic function

$$X(v) = (1 + \sigma_1^2\sigma_2^2v^2)^{-1/2}. \tag{62}$$

In order to derive the amplitude distribution of $z = xy$, we introduce $\eta = \ln z$, $\alpha = \ln x$ and $\beta = \ln y$. From $\eta = \alpha + \beta$ we obtain the distribution

$$P''(\eta)d\eta = d\eta \int P'_1(\alpha)P'_2(\eta-\alpha)d\alpha$$

$$= (2d\eta/2\pi\sigma_1\sigma_2)\int \exp[-(e^{2\alpha})/2\sigma_1^2+\alpha]\exp[-e^{2(\eta-\alpha)}/2\sigma_2^2+(\eta-\alpha)]d\alpha$$

$$= (e^\eta d\eta/2\pi\sigma_1\sigma_2)\int_{-\infty}^{\infty}\exp\{-[e^\eta/\sigma_1\sigma_2]\cosh\varepsilon\}d\varepsilon = (e^\eta d\eta/\pi\sigma_1\sigma_2)K_0(e^\eta/\sigma_1\sigma_2), \tag{63}$$

where $P'(\alpha)$ and $P'_2(\beta)$ are derived from Gaussians of dispersion σ_1 and σ_2 respectively, $\varepsilon = 2\alpha - \eta + \ln(\sigma_2/\sigma_1)$, and K is the modified zero-order Bessel function. Returning to the real variable z, we obtain from $P''(\eta)d\eta = P(z)dz$

$$P(z) = (1/\pi\sigma_1\sigma_2)K_0(z/\sigma_1\sigma_2). \tag{64}$$

A Fourier transform shows that the corresponding characteristic function is elementary:

$$Z(v) = (1 + \sigma_1^2\sigma_2^2v^2)^{-1/2}. \tag{65}$$

This is just what we wanted to prove.

Our next step is the calculation of the characteristic function of ξ. Due to the mutual dependence of x and z, the characteristic function of ξ differs from the product of the characteristic functions of x and z. We obtain instead the amplitude p.d.f.

$$I(\xi) = \int_{-\infty}^{\infty} P_1(x)P_2(\xi/x - 1)(1/|x|)dx$$

$$= [\exp(-1/2\sigma_2^2)/2\pi\sigma_1\sigma_2] \int_{-\infty}^{\infty}\exp[-x^2/2\sigma_1^2 - \xi^2/2x^2\sigma_2^2 + \xi/x\sigma_2^2]dx/|x|$$

$$= [\exp(-1/2\sigma_2^2)/2\pi\sigma_1\sigma_2] \int_{0}^{\infty}\exp[-x^2/2\sigma_1^2 - \xi^2/2x^2\sigma_2^2]\cosh(\xi/x\sigma_2^2)dx/x, \tag{66}$$

which we have written down directly, but which can also be obtained by substituting $(e^\alpha - 1)^2$ for $e^{2\alpha}$ in Eq. (63). This distribution tends to a Gaussian in the limit $\sigma_2 \to 0$, but differs slightly from a Gaussian in general. The skewness is zero, but the kurtosis exhibits a small deviation from the Gaussian amplitude p.d.f..

By performing a Fourier transform of Eq. (66) we find again that the characteristic function of the total physical thermal noise is elementary

$$X(k) = (1 + k^2\sigma_1^2\sigma_2^2)^{-1/2} \exp[-k^2\sigma_1^2/2(1 + k^2\sigma_1^2\sigma_2^2)]. \tag{67}$$

while the amplitude distribution itself can not be expressed in elementary functions. Here $\sigma_1^2 =$

$$F$$
4kTGB and $\sigma_2^2 = (\alpha A/2N) \int_f (\epsilon/\epsilon_o)^{\alpha A} d\epsilon/\epsilon]$, with B=F-f representing the bandwidth considered.

In the remaining part of this section we derive the characteristic functional of thermal noise including thermal equilibrium quantum 1/f noise in the conductance G. We first familiarize the reader with characteristic functionals in general.

3. Characteristic Functional

The complete characterization of a random process j(t) is given by its characteristic functional [39]

$$H[x(t)] = <e^{i(j,x)}>. \tag{68}$$

where j(t) is in our case the current (or voltage, or fractional conductance) fluctuation $j(t) = J(t) - <J>$, x(t) is the argument function of the functional, and the scalar product in Hilbert space is defined as

$$(j,x) = \int_0^T j^*(t)x(t)dt. \tag{69}$$

Here T is the interval of observation of the fluctuations, i.e., the length of the sample considered from the stationary random process at hand. Particularly simple, the characteristic functional of a Gaussian process is [39]

$$H_G[x(t)] = \exp[-(1/2)<(j,x)^2>]. \tag{70}$$

In particular, for thermal short-circuit current fluctuations in a resistor of conductance G described by the simple Nyquist formula with $\sigma_1^2 = 4kTGB$, the characteristic functional is

$$H[x] = \exp[-2G \int_f k_B T|x_f|^2 df] = \exp[-2k_B TGB \int_0^T |x(t)|^2 dt], \tag{71}$$

where x_f is the Fourier-transformed argument function. Here the two-sided frequency integral is limited to the allowed bandwidth B, and the time integral to the interval T of observation. Since $B \to \infty$, $k_B T$ must be replaced by $hf/[e^{hf/kT} - 1]$ and included in the frequency integral, while the time integral must also include the Fourier-transformed Planck kernel.

The characteristic functional of quantum 1/f noise affecting the conductance G has been shown [6] to be

$$H[x(\epsilon)] = \exp[-\alpha A(G^2/N) \int (\epsilon/\epsilon_o)^{\alpha A} |x(\epsilon)|^2 d\epsilon/\epsilon]. \tag{72}$$

Here αA is the infrared exponent $\alpha A = (2\alpha/3\pi)<(\Delta v/c)^2>$, which is known to enter the expression of both the basic quantum 1/f noise formula and the characteristic functional of quantum 1/f noise in two ways: as a coefficient and as an additional exponent of the frequency f. Sommerfeld's fine structure constant $\alpha = e^2/\hbar c = 1/137$ is well known, and so is the Boltzmann constant k_B. Eq. (72) gives the characteristic functional of 1/f noise for a sample containing N current carriers with an average velocity change $<(\Delta v)^2>$ in the scattering processes which determine their mobility. Since we are interested in the variable $y = \delta G/G_o$, we must replace G by 1/4 in Eq. (72).

For each value of the frequency we now use Eqs. (71) and (72), repeating the steps which led to the derivation of Eq. (65). This yields the characteristic functional of the term z=xy in Eq. (61)

24

$$Z[v(f)] = \exp[-(1/2)\int \ln(1 + \sigma_1^2\sigma_2^2v^2)df]$$
$$= \exp\{-(1/2)\int \ln[1 + 2k_BTG(\alpha A/fN)(f/f_o)^{\alpha A} v^2(f)]df\}. \qquad (73)$$

According to Eq. (61) we now have to add the Nyquist term x. Repeating for every frequency f the steps which led us to Eq. (67), we obtain now the characteristic functional of physical thermal noise ζ in the form

$$F[k(f)] = \exp\{-(1/2)\int \ln[1 + 2k_BTG(\alpha A/fN)(f/f_o)^{\alpha A}k^2(f)]df\}$$
$$\exp\{-2k_BTG\int k^2(f)[1 + 2k_BTG(\alpha A/fN)(f/f_o)^{\alpha A}k^2(f)]^{-1}df\}. \qquad (74)$$

Eq. (74) gives the characteristic functional of physical thermal noise for a sample containing N current carriers with an average velocity change $<(\Delta v)^2>$ in the scattering processes which determine their mobility, resulting in a well defined infrared exponent αA.

VII. A BRIDGE BETWEEN COHERENT AND CONVENTIONAL QUANTUM 1/f NOISE

In this section, a certain mass distribution is defined which allows arbitrary physical electronic propagators with infrared radiative corrections of any order included corresponding to given Hamiltonians and boundary conditions to be approximated by an integral over the product of this mass distribution with the corresponding well-known electronic propagator without infrared radiative corrections.

Coherent Quantum 1/f Noise Theory [14] was developed in 1982-83, nine years after Conventional Quantum 1/f Noise [1] was introduced. Both are forms of the same infrared divergence phenomenon and are described by simple universal formulas involving Sommerfeld's fine structure constant $\alpha=e^2/\hbar c$, but the coherent Q1/f formula $2\alpha/\pi f$ is particularly simple. Conventional Q1/f Noise is always present in any physical process rate or cross section, but in devices which are sufficiently large, the larger coherent Q1/f effect dominates the 1/f current noise. Since the conventional Q1/f effect is associated with individual carriers and the coherent Q1/f noise with their collective drift motion, a physical interpolation formula [15] was developed in 1985, superposing the two results in the same proportion as the kinetic and magnetic energies of the drift motion of the carriers.

As was pointed out [13] (See also the end of Sec. V above), the coherent Q1/f effect can also be derived from a quantum-electrodynamic propagator, but both this and the 1983 derivation are applicable only for a sufficiently large sample or device in which the energy of the collective magnetic field of the drift motion far exceeds the sum of the additional kinetic energies of the carriers due to their drift. For smaller samples we will attempt in this report to construct a generalization of coherent Q1/f noise which is based on the physical interpretation of a charged particle as a quantum object with indefinite energy or mass, specifically, with a fuzzy mass shell.

To achieve this objective, we represent the non-relativistic form [32] of the new quantum-electrodynamic propagator as a superposition of classical propagators, defined by an unknown mass distribution $\rho(\mu)$ which describes the fuzzy mass shell:

$$\exp\{\{\frac{im}{\hbar}[v\cdot(r\text{-}r')\text{-}(c^2+\frac{v^2}{2})(t\text{-}t')]\}\}\cdot\{\frac{im}{\hbar}[v\cdot(r\text{-}r')\text{-}(c^2+\frac{v^2}{2})(t\text{-}t')]\}^{\alpha/\pi}$$

$$= \int_0^\infty d\mu\rho(\mu)\cdot\exp\{\{\frac{i\mu}{\hbar}[v\cdot(r\text{-}r')\text{-}(c^2+\frac{v^2}{2})(t\text{-}t')]\}\}. \qquad (75)$$

25

Let $u = \frac{1}{\hbar}[\mathbf{v}\cdot(\mathbf{r}-\mathbf{r}')-(c^2+\frac{v^2}{2})(t-t')]$. This allows us to simplify the above equation, in the form

$$\int_0^{\infty} d\mu\, \rho(\mu)\cdot e^{i\mu u} = e^{imu}\cdot(imu)^{\alpha/\pi}. \tag{76}$$

When we use $\mu' = \mu - m$, the equation becomes

$$\int_{-m}^{\infty} d\mu'\, \rho'(\mu')\cdot e^{i\mu' u} = (imu)^{\alpha/\pi}. \tag{77}$$

Because $\rho'(\mu')$ is different from zero only around $\mu'=0$ or $\mu=m$, we can extend the domain of integration,

$$\int_{-\infty}^{\infty} d\mu'\, \rho'(\mu')\cdot e^{i\mu' u} = (imu)^{\alpha/\pi}. \tag{78}$$

Let us take the derivative with respect to u. This yields

$$\int_{-\infty}^{\infty} d\mu'\, \rho'(\mu')\cdot e^{i\mu' u}\cdot i\mu' = \frac{\frac{\alpha}{\pi}\cdot(im)^{\alpha/\pi}}{u^{1-\alpha/\pi}}. \tag{79}$$

We can further simplify the above equation with the notation $\mu'\cdot\rho'(\mu') = X(\mu')$ and get

$$\int_{-\infty}^{\infty} d\mu'\, X(\mu')\cdot e^{i\mu' u} = \frac{\frac{\alpha}{\pi}\cdot m^{\alpha/\pi}}{(iu)^{1-\alpha/\pi}}. \tag{80}$$

We can determine $X(\mu')$ by taking the Fourier transformation of the right hand side,

$$X(\mu') = \int_{-\infty}^{\infty} du\, \frac{\frac{\alpha}{2\pi^2}\cdot m^{\alpha/\pi}}{(iu)^{1-\alpha/\pi}}e^{iu\mu'} = \frac{\alpha m^{\alpha/\pi}}{2\pi^2 i^{1-\alpha/\pi}} \int_{-\infty}^{\infty} du\, \frac{e^{-iu\mu'}}{u^{1-\alpha/\pi}} \tag{81}$$

$$= \frac{\alpha m^{\alpha/\pi}}{2\pi^2 i^{1-\alpha/\pi}} \left(\int_{-\infty}^{0} du\, \frac{\cos(\mu'u)+i\sin(\mu'u)}{u^{1-\alpha/\pi}} + \int_0^{\infty} du\, \frac{\cos(\mu'u)+i\sin(\mu'u)}{u^{1-\alpha/\pi}} \right)$$

$$(u'=-u) = \frac{\alpha m^{\alpha/\pi}}{2\pi^2 i^{1-\alpha/\pi}} \left(\int_0^{\infty} d(-u') \frac{\cos(-\mu'u')+i\sin(-\mu'u')}{(-u')^{1-\alpha/\pi}} + \int_0^{\infty} du\, \frac{\cos(\mu'u)+i\sin(\mu'u)}{u^{1-\alpha/\pi}} \right)$$

$$= \frac{\alpha m^{\alpha/\pi}}{2\pi^2 i^{1-\alpha/\pi}} \left(\int_0^{\infty} du'\, \frac{-\cos(\mu'u')+i\sin(\mu'u')}{u'^{1-\alpha/\pi}}\cdot(-1)^{1-\alpha/\pi} + \int_0^{\infty} du\, \frac{\cos(\mu'u)+i\sin(\mu'u)}{u^{1-\alpha/\pi}} \right)$$

$$= \frac{\alpha m^{\alpha/\pi}}{2\pi^2 i^{1-\alpha/\pi}} \left[(1-(-1)^{1-\alpha/\pi})\cdot\int_0^{\infty} du\, \frac{\cos(\mu'u)}{u^{1-\alpha/\pi}} + i(1+(-1)^{1-\alpha/\pi})\cdot\int_0^{\infty} du\, \frac{\sin(\mu'u)}{u^{1-\alpha/\pi}} \right]$$

$$= \frac{\alpha m^{\alpha/\pi}}{2\pi^2 i^{1-\alpha/\pi}} \left[(1-(-1)^{1-\alpha/\pi})\cdot\frac{\Gamma(\alpha/\pi)}{\mu'^{\alpha/\pi}}\cdot\cos(\alpha/2) + i(1+(-1)^{1-\alpha/\pi})\cdot\frac{\Gamma(\alpha/\pi)}{\mu'^{\alpha/\pi}}\cdot\sin(\alpha/2) \right] \tag{82}$$

26

(for $\mu' > 0$), and

$$=\frac{\alpha m^{\alpha/\pi}}{2\pi^2 i^{1-\alpha/\pi}}\left[(1-(-1)^{1-\alpha/\pi})\cdot\frac{\Gamma(\alpha/\pi)}{\mu'^{\alpha/\pi}}\cdot\cos(\alpha/2) - i(1+(-1)^{1-\alpha/\pi})\cdot\frac{\Gamma(\alpha/\pi)}{\mu'^{\alpha/\pi}}\cdot\sin(\alpha/2)\right] \qquad (83)$$

(for $\mu' < 0$).

Because both $1+(-1)^{1-\alpha/\pi}$ and $\sin(\alpha/2)$ are much smaller than $1-(-1)^{1-\alpha/\pi}$ and $\cos(\alpha/2)$, we can just use

$$X(\mu') = (1-(-1)^{1-\alpha/\pi})\,\frac{\alpha\Gamma(\alpha/\pi)\cos(\alpha/2)}{2\pi^2 i^{1-\alpha/\pi}}(\frac{m}{\mu'})^{\alpha/\pi} . \qquad (84)$$

for all practical purposes. We thus conclude that the mass distribution function has to be

$$\rho(\mu) = \frac{\alpha\Gamma(\alpha/\pi)\cos(\alpha/2)}{\pi^2 i^{1-\alpha/\pi}}\cdot\frac{m^{\alpha/\pi}}{(\mu-m)^{1+\alpha/\pi}} . \qquad (85)$$

This is a remarkable result. It allows us to approximate the effect of infrared radiative corrections on any electronic propagator by multiplying it by $\rho(\mu)$ and integrating over μ as was done with the free particle propagator on the right-hand side of our first equation above. The result will represent an approximation of the physical electron's propagator corresponding to the problem at hand, i.e., an approximation of the physical propagator including the infrared radiative corrections, which corresponds to the given potential in which the electron has to move, and which satisfies the given boundary conditions.

VII. APPLICATION OF HIGH ε PARAMAGNETIC AND FERROELECTRIC MATERIALS TO HIGH-TRANSCONDUCTANCE HFETs WITH LOW NOISE AND LOW GATE CURRENT

1. Introduction

The main problem in high-transconductance FETs is the presence of a considerable gate leakage current that loads the input and reduces the power amplification coefficient. The problem has become particularly serious in InGaAs Heterostructure FETs.

Indeed, to achieve a high transconductance, the gate capacitance must be high, and the gate insulation must be thin. This leads to tunneling currents through the gate insulation.

A detailed examination of the quantum-mechanical tunneling problem by these authors in cooperation with F. Schuermeyer in 1993-1996 shows that the only way to reduce the gate tunneling current without sacrificing the gate capacitance is to use materials with high dielectric constant ε_r as insulators under the gate.

It is obvious that only amorphous ferroelectric materials with negligible remanent polarization and high coercive field are useful if we want to avoid the hysteresis effect, and are interested only in suppression of the leakage currents in high transconductance devices. For certain applications, hysteresis in the response of the device is desirable, and should be achievable by slight modifications in the fabrication process. The present report analyzes the possibility of using ferroelectric and paraelectric high ε gate insulators, including also noise considerations, in particular quantum 1/f noise.

2. General Considerations

An increased gate capacitance is particularly desirable at lower frequencies, because it leads

27

to higher transconductances of the FET, without compromising its desirable large input impedance. At high and ultrahigh frequencies, however, a very large gate capacitance C is less desirable, because it essentially shorts the gate to the channel and requires large capacitive gate currents and signal power input levels at the achievable f_τ and f_{max} values. The natural solution that allows for a smaller frequency dependence of the input admittance $j\omega C$ is a ferroelectric gate insulation. Indeed, at low frequencies, it could increase the gate capacitance and device transconductance by a factor of 10^2, while at higher frequencies, where such a large capacitance could be harmful, the dielectric constant decreases to intermediate values, allowing for operation at the highest frequencies with a reasonable input impedance. This is the main advantage of a ferroelectric gate insulation.

Unfortunately, the ferroelectric introduces its own resonances and their characteristic frequencies, as well as dissipation. Furthermore, if leakage through the ferroelectric is still occurring, it leads to a normalized quantum 1/f noise coefficient larger by a factor of 10^6 than what we would get without piezoelectric coupling of the current carriers.

A possible way for reducing the remaining frequency dependence of the gate capacitance is the use of two or more ferroelectric layers. This introduces additional resonances and resonances corresponding to the space-charge relaxation at the interfaces. However, in return, each of these resonances could be weighted down so that the resulting frequency dependence will just present small nonuniformities which cause negligible spectral distortion in amplifiers.

3. History

The effect of ferroelectric polarization on insulated-gate thin film transistor parameters was first studied by Zuleeg and Wieder [40] as a device for non-volatile memory design. They applied a 1 mm thick film of ferroelectric TGS (tri-glicine-sulphate) on one side of a 5,000Å CdS film as gate insulation, the other side of the film being insulated by 1000Å of SiO_2 from an Al gate. Gold was used for the gate applied to the TGS, the source and the drain contacts. Depending on the polarization state of the TGS, controlled by the gold gate voltage, and by its previous voltage history, one gets various sets of drain characteristics. In the metal-ferroelectric semiconductor structure, proposed later by Wu [41], a thin film of ferroelectric $Bi_4Ti_3O_{12}$ was replacing the oxide of a MOSFET. This was suggested as a new ferroelectric memory device. The materials PZT, i.e., $PbZr_xTi_{1-x}O_3$ [42] and $LiNbO_3$ [43] were investigated as ferroelectric gate insulators, as well as other materials [44]. However, all these materials contain oxygen, and will cause oxidation of the compound semiconductors.

On the other hand, the nature of the leakage current was investigated in HFETs by Schuermeyer et. al., [45]-[46]. They focused primarily on the thermal activation of carriers from the channel over the barrier separating them from the gate. These authors found that the density of the thermal activation current reached a maximum at an intermediary region, closer to the drain than to the source. In the present report, we illustrate the application of ferroelectric or high ε materials to the case of the InGaAs/AlGaAs/GaAs and InGaAs/InAlAs/InP enhancement-mode HFETs fabricated and studied by Schuermeyer et. al., [45]-[46].

4. Approach

We will consider the ferroelectric material $BaMgF_4$ as a leading candidate for coating the barrier layer, applying it in its amorphous form at 450° C on the external AlGaAs barrier layer, separating the channel from the gate of the HFET. In this form it has negligible hysteresis and is characterized by a dielectric constant $\varepsilon_i=35$. The deposition temperature is not too high for the HFET. The AlGaAs barrier thickness d can be reduced to 15 nm and the $BaMgF_4$ layer needs to be only 20 nm thick. Fig. 1 and 2 show the approximate device structure and the conduction band configuration for an n-channel HFET.

To further clarify our approach, we use the simple FET expression for the intrinsic
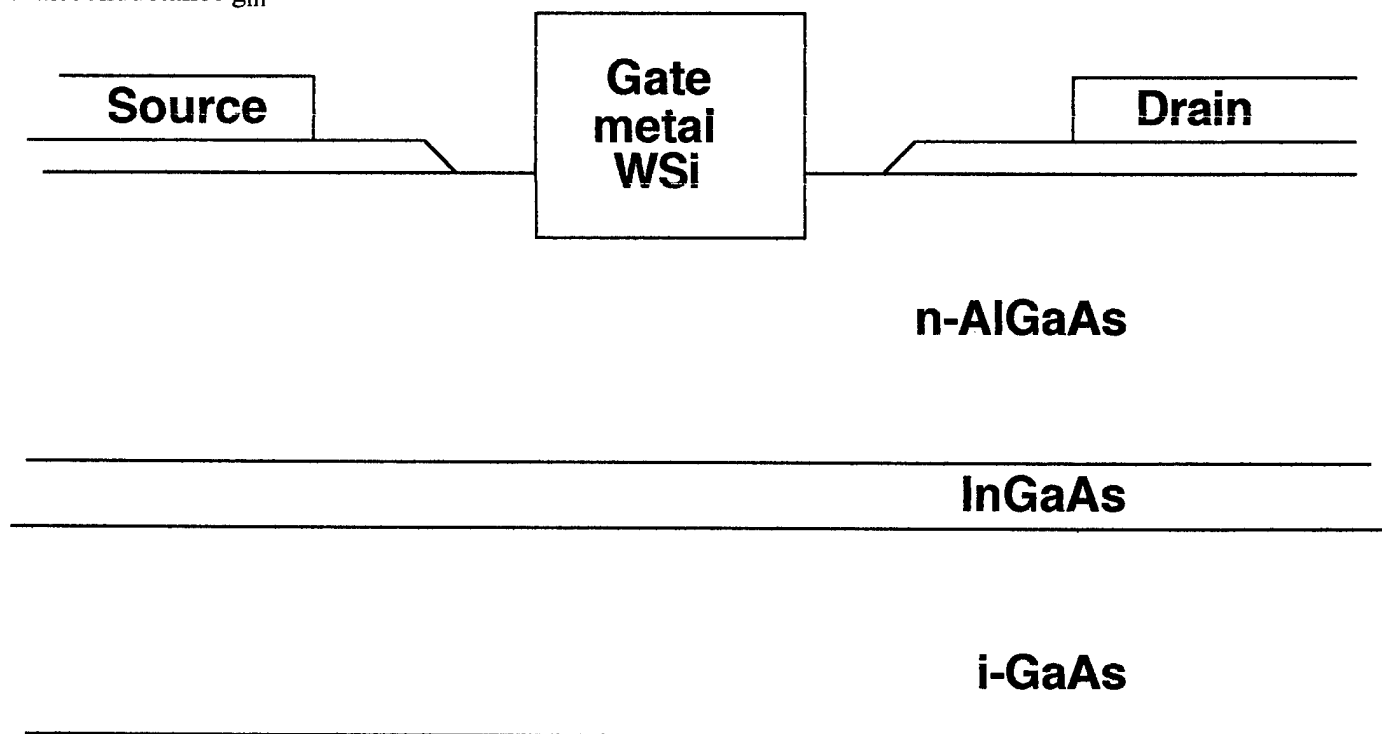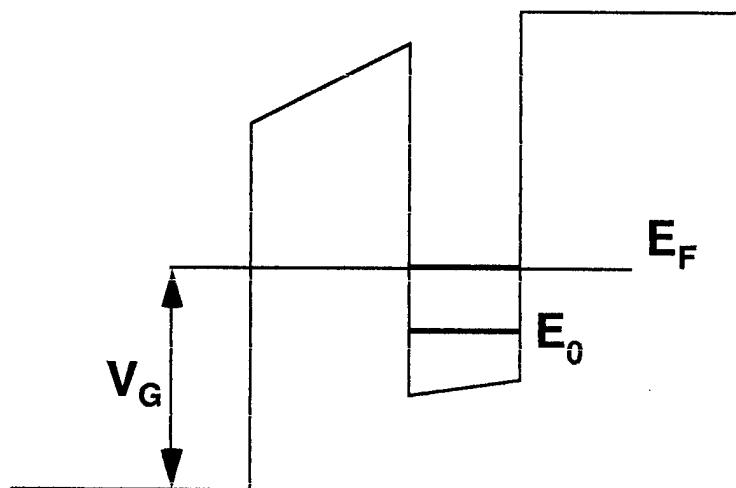
transconductance g_m

Fig. 1': HFET structure.

Fig. 2': HFET Band Structure

$$g_m = \frac{C_G}{t_c}, \quad \text{with} \quad C_G = \frac{\varepsilon LW}{t_{ins}} \tag{86}$$

$$\text{and } t_c = \frac{L^2}{2\mu V_D} \text{ for low field, or } t_c = \frac{L}{v_m} \text{ for high field.} \tag{87}$$

Here C_G is the gate capacitance, t_c the effective channel transit time, ε the effective permittivity of the gate capacitance, L the gate length, W its width, t_{ins} the effective distance between gate and channel, equivalent with a total insulation thickness, μ the effective channel mobility, V_D the source-drain voltage, and v_m the maximal drift velocity obtained in the high field regime of the channel.

From Eqs. (86) and (87) we see that by increasing t_{ins} by a factor λ and ε by a factor λ^4, g_m will increase by a factor of λ^3. At the same time the leakage current caused by tunneling through the barrier will become negligible for all practical purposes for $\lambda \geq 2$, because the tunneling probability T«1 will be replaced by $\leq T^2$. Indeed, an additional decrease of the gate current will be caused by the reduction of the electric field present throughout the barrier.

The unit current gain frequency, f_τ, is not affected, being approximated by

$$f_\tau = 1/2\pi t_c. \tag{88}$$

However, the maximum frequency of oscillation, f_{max}, is given by

$$f_{max} = (f_\tau/2)(g_m/g_{out})^{1/2}, \tag{89}$$

where g_{out} is the output conductance that is not affected by C_G or by λ. The maximum frequency of oscillation is therefore increased by $\lambda^{3/2}$, provided there is no decrease in ε at $f=f_{max}$. For instance, with $\lambda=1.41$, increasing t_{ins} 1.41 times and ε 4 times will increase g_m 2.82 times, f_{max} 1.65 times and stop the gate current. Actually, there will be a considerable decrease of ε at high frequencies, and therefore, we expect f_{max} to increase less than predicted by the factor $\lambda^{3/2}$.

5. BaMgF$_4$ Technology

The ferroelectricity of BaMgF$_4$ was discovered in 1969. However, this material was not fabricated as a thin film till 1989, and was first deposited on Si surfaces to generate ferroelectric memory FETs [47]. It has been found that BaMgF$_4$ grown on GaAs or AlGaAs (100) surfaces at 450°C is amorphous [48]. This film does not exhibit hysteresis, but is a paraelectric insulator with a relative dielectric constant ε_r of 35. The substrate was (100) n-type GaAs at 450°C. The growth rate was 0.4 μm/h.

At temperatures of 500-600°C polycrystalline ferroelectric films exhibiting hysteresis were grown, with a (140) orientation. Their coercive field was about 200kV/cm and the remanent polarization P_r about 1.3 μC/cm^2. For monocrystalline material the expected value of P_r is 4 μC/cm^2.

In order to obtain high-g_m HFETs with truly negligible gate currents, we therefore recommend choosing the factor λ defined in Sec. 4 to be $\sqrt{2}$. We thus obtain a transconductance increased by a factor of $2\sqrt{2}$, a total barrier thickness increased by a factor of $\sqrt{2}$, and therefore a negligible gate current. Practically, this is achieved by properly structuring the barrier grown on the undoped GaAs channel. First a 5 nm undoped AlGaAs spacer layer is deposited on the channel, then 10 nm of n-type AlGaAs, followed by 20 nm of amorphous BaMgF$_4$, and by the metal of the gate electrode, e.g., Al.

By varying the growing temperature and speed in the interval of 450-495°C and around 0.4

μm/h, we may be able to achieve a useful further increase in ε without detrimental hysteresis effects.

6. 1/f Noise

The 1/f noise of the 2-DEGrees-of-freedom-electrons in the conducting InGaAs channel is determined by the conventional quantum 1/f formula for polar optical scattering at 300K, or for the mixture of polar optical phonon, longitudinal acoustical phonon, piezoelectric, and lattice defect scattering at 70K. The spectral density S of fractional quantum 1/f fluctuations $\delta\Gamma/\Gamma$ of the electron scattering rate Γ in a process with velocity change Δv of the electrons is

$$S_{\delta\Gamma/\Gamma}(f) = 2\alpha A/fN = (4\alpha/3\pi fN)(\Delta v/c)^2. \tag{90}$$

The fractional quantum 1/f fluctuation $\delta\Gamma/\Gamma$ of the electron scattering rate Γ on a polar optical phonon of momentum $\hbar q$ and energy $\hbar\omega_q \approx \omega_0$ is given by the spectral density

$$S_{\delta\Gamma/\Gamma}(f) = (4\alpha/3\pi fN)<(\hbar q/m_{eff}c)^2> = (4\alpha/3\pi fN)2<(\hbar k/m_{eff}c)^2>. \tag{91}$$

Here we have estimated the average quadratic momentum change of the electrons, resulting from the momentum $\hbar q$ of the optical phonon to be $2(\hbar k)^2$, because the momentum transfer to electrons of momentum $\hbar k$ is known [46] to be between the limits $\hbar q_{min}= \hbar\{-k+[k^2 + 2m_{eff}\omega_0/\hbar]^{1/2}\}$ and $\hbar q_{max}= \hbar\{k+[k^2 + 2m_{eff}\omega_0/\hbar]^{1/2}\}$. With $<(\hbar k/m_{eff})^2> =3kT/m_{eff}$ and $m_{eff}= 0.068m_o$, Eq. (91) yields a spectral density

$$S_{\delta\Gamma/\Gamma}(f) = 1.8 \cdot 10^{-8} /fN = S_{\delta\mu/\mu}(f) = S_{\delta I/I}(f), \tag{92}$$

where I is the source to drain current, and N the number of carriers in the channel. The expected rms drain current fluctuation amplitude is thus $1.34 \cdot 10^{-4} I_d/N\sqrt{f}$. Both through N and through the drain current I_d this simple result depends on the applied gate voltage V_G.

7. Conclusions

The preceding discussion indicates that a paraelectric or hysteresis-free ferroelectric gate insulation is ideal for special HFETs meeting bandwidth requirements from 0 to 100 GHz. It allows total suppression of gate leakage currents, while also assuring a large increase in the transconductance of the device at frequencies under 100 MHz, where the permittivity is still high.

The gradual decrease of ε in the UHF region is actually very useful, since it limits the free fall of the input impedance $(j\omega C)^{-1}$ of the device to zero, which would load the source excessively.

Finally, the lower temperature BaMgF$_4$ technology avoids oxidation and degradation of the compound semiconductors, and a further improvement in ε through mobile ferroelectric micro-domains is possible by optimizing the growing conditions.

The author is indebted to F. Schuermeyer for suggesting the research for elimination of gate currents and for many helpful discussions.

IX. TWO-DIMENSIONAL ALL-OPTICAL PARALLEL-TO SERIES TDM AND DE-MULTIPLEXING BY SPECTRAL-HOLOGRAPHIC METHODS

All-optical one-dimensional parallel-to serial conversion by holographic one-dimensional space-to time frequency encoding was recently introduced [49], along with the previously known series-to-parallel transformation. However, the large discrepancy between the Gbit/s capacity of coaxial cables and the Tbit/s rates achievable in optical fibers for photonic networks, requires the multiplexing of roughly 10^3 incoming conventional signals in a single optical fiber. This requires harnessing of the full power of Fourier-optical holographic methods, by using both dimensions of optical wavefronts for data processing. The processor system we propose consists of two independent optical channels C_t and C_s for carrying temporal signals and spatial information, both in its parallel-to-series (Fig. 1") and in its series-to-parallel (Fig. 2") parts. C_t is shown with continuous lines, representing ultra-short pulsed beams, while C_s is shown with dotted rays, using longer pulses.

C_t passes the ultrashort pulse wave-fronts through a blazed 2-dimensional reflecting diffraction grating G_1 which is described below, followed by a lens L_1 of focal length F, a real-time hologram H in its focal plane, an identical lens L_2, and a second, similar, 2-D reflection grating G_2, with a distance F between each of these 5 elements on their common optical axis.

C_s is an optical Fourier transform channel which inputs the modified image of a rectangular array of sources. C_s introduces this image through the semi-transparent mirror M together with a reference beam. They are introduced backwards through the lens L_2, creating a Fourier-transform hologram H which in turn acts on the forward-propagating C_t beam, splitting it up in a number of temporally displaced beams equal with the number of sources present in the input of C_s. The sum of these beams is Fourier-transformed back to the time-domain, yielding the desired *serial output* of the given parallel data input. The modification hikes line intervals n times.

First a general analysis of the 2-D parallel-to-series converter will be presented, and then a brief discussion of the corresponding receiver. The multiplexer works in two steps.
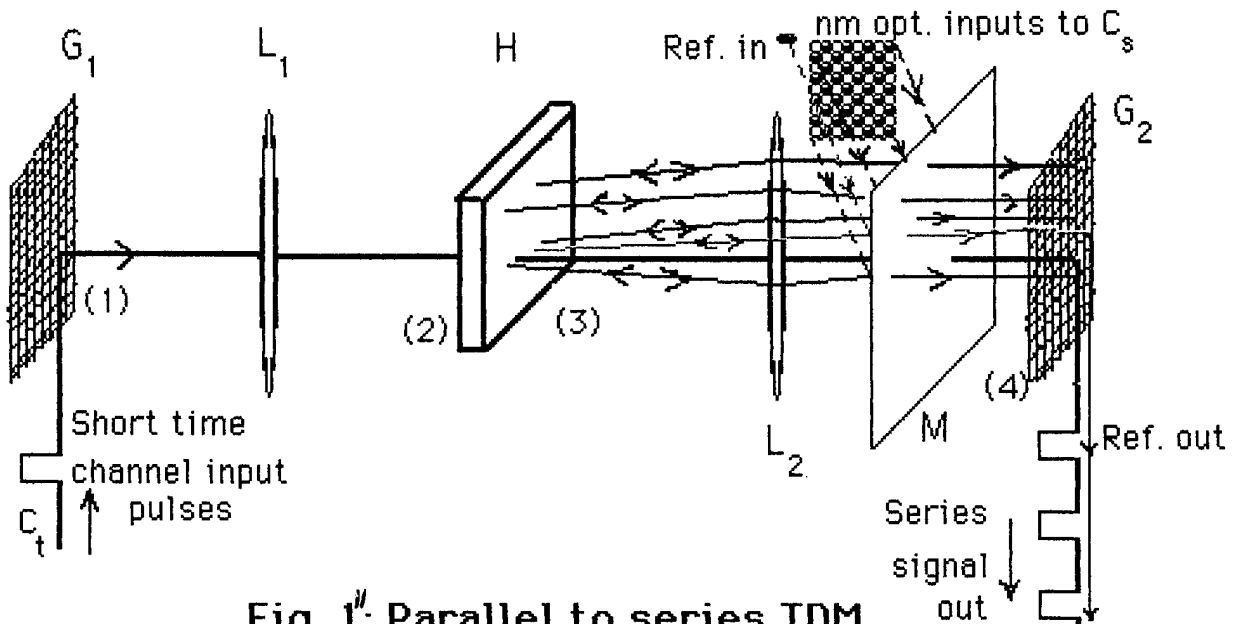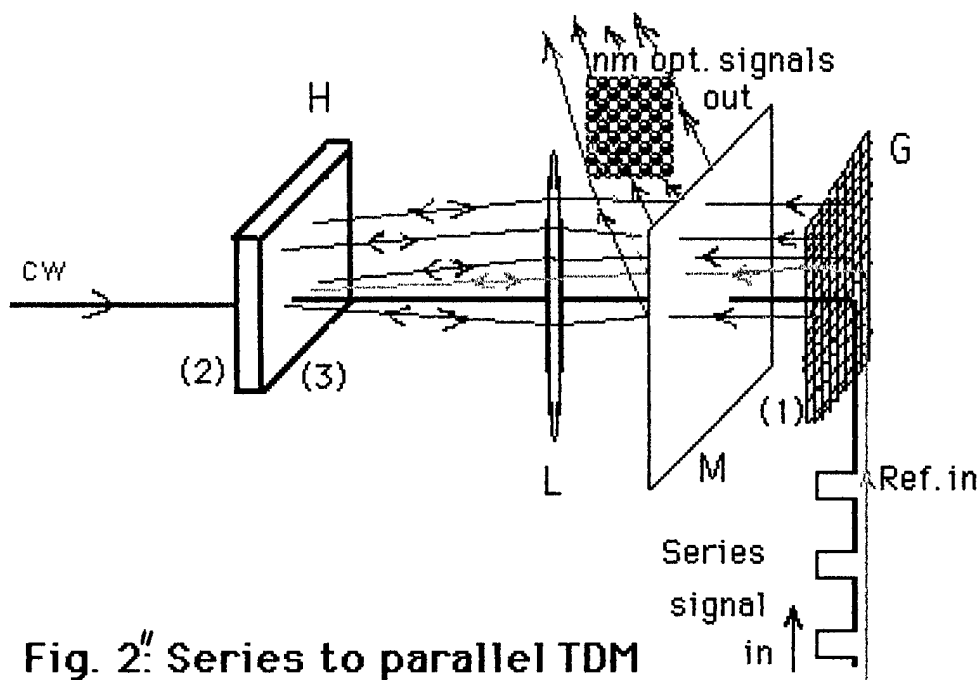

Fig. 1": Parallel to series TDM
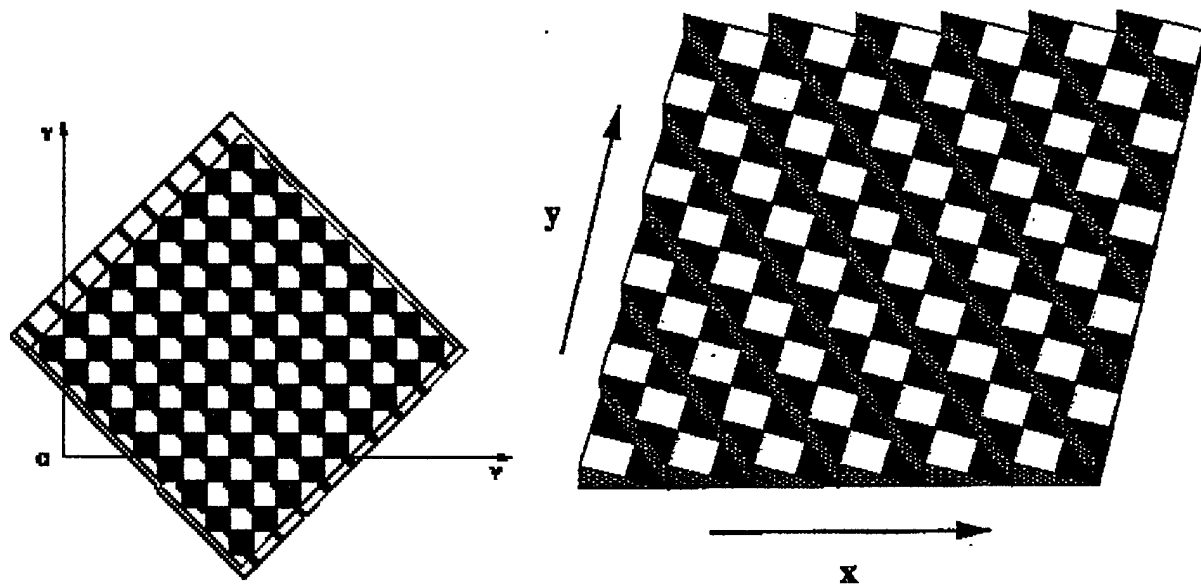
Fig. 2: Series to parallel TDM

Fig. 3: Two-dimensional blazed diffraction grating, front view and perspective.

1) In a first step, starting from a single mode-locked laser, a 2-dimensional manifold of N=n×m coherent beams is created by multiple beam-splitting, along with a reference beam. By synchronized sampling and birefringent synchronous modulation, we transfer the information from each one of the N incoming coaxial cables to one of the N beams, in the form of pulses of length τ. The reference beam always carries the standard, unmodulated pulse generated by the laser. Part of the reference beam is separated by a beam splitter and is then re-shaped [50,51] for C_t to be ultra short of duration τ_0 ($<<\tau$, up to 10^{-3} τ, of the order of the reciprocal carrier bandwidth, a few tens

33

of femtoseconds). The rest of the reference beam separated by the beam splitter goes to the C_S channel together with the N modulated beams. The first step thus creates *a rectangular array of luminous sources with n columns and m rows plus the reference beam, which yield the (τ) input beam to C_S, and an ultrashort sequence of pulses which yields the (τ₀) input beam to C_t.* The input to C_t is thus a regular sequence of pulses in time, of the form

$$s(t) = p(t-t_0) \exp(j\omega_c t), \qquad (93)$$

with Fourier transform

$$P(\omega-\omega_c)\exp[-j(\omega-\omega_c)t_0], \qquad (94)$$

where $P(\omega)$ is the Fourier transform of $p(t)$.

2) In the second step, this input beam passes through C_t. Let the temporal transfer function of C_t be $H(\omega)$. Then the output spectrum will be

$$H(\omega)P(\omega-\omega_c)\exp[-j(\omega-\omega_c)t_0]. \qquad (95)$$

To calculate $H(\omega)$, we calculate the output resulting from the passage of a monochromatic input $\exp[j(\omega t - \mathbf{k} \mathbf{r})$ through C_t. Let $\mathbf{k}$ be incident on the 2-D diffraction grating located in the xy plane with directing cosines α and β to the x and y axes. The blazed 2-D diffraction grating is obtained by applying a squared lattice chess board-like black deposit on a 1-D blazed diffraction grating at 45° to the diffraction grating, i.e., so that the x and y axes of the applied chess board are at 45° from the groves of the 1-D blazed grating (Fig. 3). The lattice constant of the applied chess-board lattice is twice the side of any white or black field on the chess board, and equals the constant of the original blazed lattice times $2^{1/2}$. The diffracted optical field (Fig. 1') generated by the monochromatic input right after the plane P₁ of the grating is

$$s_1(x,y; \omega) = \exp[-j(\omega-\omega_c)(\alpha x+\beta y)/c] \, w(x,y), \qquad (96)$$

where $w(x,y)$ is the pupil function of the grating. After passage through the lens L₁ the optical field in plane P₂ right before the hologram is the Fourier transform of the field in Eq. (96), given by

$$s_2(\xi,\eta; \omega) = W[\xi+\alpha(\omega-\omega_c)/2\pi c, \, \eta+\beta(\omega-\omega_c)/2\pi c], \qquad (97)$$

where $W(\xi,\eta)$ is the spatial Fourier transform of $w(x,y)$. The wave numbers ξ and η are expressed in terms of the spatial Cartesian coordinates X and Y in P₂ by $\xi=\omega X/2\pi cF$ and $\eta=\omega Y/2\pi cF$. We note parenthetically that, as indicated by Eq. (97), an optical pulse introduced into the system will have its various Fourier components spatially dispersed along the diagonal of the Fourier transform plane, each occupying an area determined by the function $W(\xi,\eta)$.

We now take into account that a spatial Fourier transform hologram of the above-mentioned rectangular n×m input array has been independently recorded by C_S in the hologram H of Fig. 1''. This hologram is a superposition of the n×m holograms of the individual luminous sources present in the rectangular input array, with amplitudes $A_{\mu\nu}$ corresponding to the bit of information carried by the channel μν to be multiplexed. This hologram serves as a temporal frequency filter with transmittance

34

$$t(\xi,\eta) = \sum_{\mu=1}^{m} \sum_{\nu=1}^{n} A_{\mu,\nu}\exp[j2\pi(\omega_w/\omega)(\nu\Delta_x\xi+\mu\Delta_y\eta)], \qquad (98)$$

where Δ_x is the geometrical distance between columns and Δ_y is the modified distance between the rows in the regular input array fed into C_s, whereas ω_w is the frequency of the writing field used for recording the hologram, in our case ω_c. It is necessary to take $\Delta_y \geq n\Delta_x$, and suitable to choose, e.g., $\Delta_y = (n+1)\Delta_x$. This is achieved with the help of a convergent cylindrical magnifying lens placed in front of the rectangular array of light sources, with its cylindrical axis parallel to the x-axis, which would cause the separation between rows to appear larger. In addition, we assume $(n+1)m\Delta_x+c\tau_0 \leq c\tau$.

Returning now to C_t, right after passage through the hologram, the optical field in P3 will be

$$s_3(\xi,\eta; \omega) = s_2(\xi,\eta; \omega)\, t(\xi,\eta). \qquad (99)$$

After passage through L_2, the field in plane P4 is given by a second spatial Fourier transform which yields

$$s_4(x,y; \omega) = \sum_{\mu=1}^{m} \sum_{\nu=1}^{n} A_{\mu,\nu}w[-x+\nu\Delta_x, -y+\mu\Delta_y]$$
$$\times\exp[(j/c)(\omega-\omega_c)[\alpha(x-\nu\Delta_x(\omega_w/\omega)) + \beta(y-\mu\Delta_y(\omega_w/\omega))]. \qquad (100)$$

This field is diffracted by the 2-D grating G_2 and yields the output field propagating in the k'' or z'' direction

$$s_5(x'',y''; \omega) = \sum_{\mu=1}^{m} \sum_{\nu=1}^{n} A_{\mu,\nu}w[-x''+\alpha''\nu\Delta_x, -y''+\beta''\mu\Delta_y]$$
$$\times\exp[(j/c)(\omega-\omega_c)(\omega_w/\omega)(\alpha\nu\Delta_x + \beta\mu\Delta_y)] = H(\omega). \qquad (101)$$

This is the temporal transfer function of the system. Here α'' and β'' are directing cosines of the outgoing wave vector k''. Assuming $\Delta_y = (n+1)\Delta$ and $\Delta=\Delta_x$,

$$H(\omega) = \sum_{\mu=1}^{m} \sum_{\nu=1}^{n} A_{\mu,\nu}w[-x''+\alpha''\nu\Delta_x, -y''+\beta''\mu\Delta_y]$$
$$\times\exp\{j(\Delta/c)(\omega-\omega_c)(\omega_w/\omega)[\alpha\nu + \beta\mu(n+1)]\} \qquad (102)$$

The temporal output function allows the determination of the serial output of the multiplexer as the Fourier transform of Eq. (95)

$$s_0(x'',y''; t) = [\sum_{\mu=1}^{m} \sum_{\nu=1}^{n} A_{\mu,\nu}w[-x''+\alpha''\nu\Delta_x, -y''+\beta''\mu\Delta_y]p(t-t_0 -r\delta t)]\exp(j\omega_c t). \qquad (103)$$

Here $r = \nu + \mu(\beta\Delta_y/\alpha\Delta_x) = \nu + \mu(\beta/\alpha)(n+1)$; for $\alpha=\beta$, $r = \nu + \mu(n+1)$. The interval δt was defined as $\alpha\Delta_x/c$. The ratio ω_w/ω was approximated by 1 which is reasonable for not too large bandwidths, but may lead to errors in our case. These errors should be further investigated.

Eq. (103) shows that the parallel-to-series or multiplexing operation was performed. Along with the series signal, the non-diffracted portion of the readout beam coming from the hologram H

in Fig. 1 is also transmitted to the receiver as a reference signal.

In principle, all beams could be reversed. This observation makes the description and operation of the de-multiplexer shown in Fig. 2 straightforward. A hologram is recorded at the receiver site between the incoming serial signal shown by Eq. (103) and the received reference signal, both having first been diffracted in reflection by the identical diffraction grating G. This real time hologram is modulating the cw monochromatic readout wave front coming from the left in Fig. 2 and passing through the hologram, thereby creating N=n×m beams. The result is thus a two-dimensional n×m parallel optical output which is extracted with the help of the semi-transparent mirror M and projected on a n×m array of outgoing optical fibers, or on a similar array of photodetectors.

X. REFERENCES

[1] P.H. Handel, "1/f Noise - an 'Infrared' Phenomenon". Phys. Rev. Letters **34**, 1492-1494 (1975); "Nature of 1/f Phase Noise", Phys. Rev. Letters 34, 1495-1498 (1975); "Quantum Approach to 1/f Noise", Phys. Rev. **22A**, 745-757 (1980).

[2] P.H. Handel, "Quantum Approach to 1/f Noise" Phys. Rev. **A22**, 745 (1980).

[3] P.H. Handel: "Infrared Divergences, Radiative Corrections and Bremsstrahlung in the Presence of a Thermal Equilibrium Radiation Background", Phys. Rev. **A38**, 3082-3085 (1988).

[4] P.H. Handel: "Quantum 1/f Noise in the Presence of a Thermal Radiation Background", Proc. II Internat. Symposium on 1/f Noise, C.M. Van Vliet and E.R. Chenette Editors, p.42-54, Orlando 1980.(University of Florida, Gainesville Press), p.96-110.

[5] T.S. Sherif and P.H. Handel: "Unified Treatment of Diffraction and 1/f Noise", Phys. Rev. **A26**, p.596-602, (1982).

[6] P.H. Handel and D. Wolf: "Characteristic Functional of Quantum 1/f Noise", Phys. Rev. **A26**, 3727-30 (1982).

[7] P.H. Handel and T. Sherif: "Direct Calculation of the Schroedinger Field which Generates Quantum 1/f Noise", Proc. VII Int. Conf. on Noise in Physical Systems and III Int. Conf. on 1/f Noise, Montpellier, May 17-20, 1983, V.M. Savelli, G. Lecoy and J.P. Nougier Editors, North-Holland Publ. Co. (1983) p. 109-112.

[8] P.H. Handel: "Effect of a Finite Mean Free Path on Quantum 1/f Noise", Proc. of the IX International Conference on Noise in Physical Systems, Montreal (Canada), 1987, C.M. Van Vliet Editor, World Scientific Publ. Co., 687 Hartwell Str., Teaneck, NJ 07666, pp. 365-372, pp. 419-422..

[9] G.S. Kousik, C.M. van Vliet, G. Bosman and P.H. Handel: "Quantum 1/f Noise Associated with Ionized Impurity Scattering and Electron-phonon Scattering in Condensed Matter", Advances in Physics **34**, p. 663-702, (1986); see also the continuation: [10'] G.S. Kousik et al., "Quantum 1/f Noise Associated with Intervalley Scattering in Nondegenerate Semiconductors" Phys. Stat. Sol. (b) **154**, 713 (1989).

[10] P.H. Handel and C. Eftimiu, "Survival of the Long Time Correlations in 1/f Noise", Proc. of the Symposium on 1/f Fluctuations, Tokyo (Japan) July 11-13, 1977, Tokyo Institute of Technology Press, pp.183-186(1977).

[11] P.H. Handel, Archiv für Elektronik u. Übertr. **43**, 261 (1989).

[12] A. van der Ziel: "Unified Presentation of 1/f Noise in Electronic Devices; Fundamental 1/f Noise Sources", Proc. IEEE **76**, 233-258 (1988); also 'Noise in Solid State Devices and Circuits", J. Wiley & Sons, New York 1986, Ch. 11, pp. 254 - 277.

[13] P.H. Handel, "Fundamental Quantum 1/f Noise in Small Semiconductor Devices", IEEE Trans. on Electr. Devices **41**, 2023-2033 (1994).

[14] P.H. Handel, "Any Particle Represented by a Coherent State Exhibits 1/f Noise", Proc. VII Int. Conf. on Noise in Physical Systems and III Int. Conf. on 1/f Noise, Montpellier, May 17-20, 1983, V.M. Savelli, G. Lecoy and J.P. Nougier Editors, North-Holland Publ. Co.

(1983), p. 97-100.

[15] P.H. Handel , "Coherent States Quantum 1/f Noise and the Quantum 1/f Effect", Proc. VIII Int. Conference on Noise in Physical Systems and IV Int. Conference on 1/f Noise, Rome, September 1985, A. D'Amico and P. Mazzetti Editors, North Holland Publishing Co., pp. 465-468.

[16] P.H. Handel , "Coherent Quantum 1/f Effect in Second Quantization", *5th van der Ziel Symposium on Quantum 1/f Noise and Other Low Frequency Fluctuations in Electronic Devices*, May 22-23, 1992, St. Louis, MO, AIP Conference Proceedings No. 282, P.H. Handel and A.L. Chung, Editors, pp. 28-30 (1993).

[17] J.R. Vig and F.L. Walls: "Fundamental limits on the frequency instabilities of quartz crystal oscillators." Proc. 48th Annual Frequency Control Symposium, pp. 506-523, 1994.

[18] P.H. Handel: "Nature of 1/f frequency fluctuation in quartz crystal resonators", Solid State Electronics $2\,2$, p. 875 (1979).

[19] J.J. Gagnepain and J. Uebersfeld: "1/f Noise in quartz crystal resonators." Proc. of the 1st Symposium on 1/f fluctuations, Sasakawa hall, Tokyo, Japan, July 11-13, 1977, pp. 173-182, Toshimitsu Musha Editor, Tokyo Institute of Technology Press, 1977.

[20] T.E. Parker: "1/f Frequency fluctuations in quartz acoustic resonators." Proc. 39th Ann. Freq. Control Symp., pp. 97-106, 1985; Appl. Phys. Letters, Febr. 1, 1985.

[21] P.H. Handel, Second Annual Report, AFOSR Grant #89-0416/July 15, 1991, page 8.

[22] F.L. Walls, P.H. Handel, R. Besson and J.J. Gagnepain: "A new model relating resonator volume to 1/f noise in BAW quartz resonators." Proc. 46th Annual Frequency Control Symposium, pp. 327-333, 1992.

[23] P.H. Handel: Analysis of quantum 1/f effects in frequency standards. Proc. 48th Ann. Freq. Contr. Symp., pp. 539-540, 1994.

[24] P.H. Handel: "!/f Noise universality in high-technology applications." Proc. 48th Ann. Freq. Contr. Symp., pp. 8-21, 1994.

[25] T.E. Parker and D. Andres: "1/f Noise in surface acoustic wave resonators." Proc. 48th Ann. Freq. Contr. Symp., pp. 530-538, 1994.

[26]T.E. Parker, D. Adres, J.A. Greer and G.T. Montress: "1/f Noise in etched groove surface acoustic wave resonators." IEEE Transactions on Ultrasonics, Ferroelectrics and Frequency Control, <u>41</u>, 853-862 (1994).

[27] J.D. Dollard, J. Math. Phys. **5**, 729 (1965).

[28] P.P.Kulish and L.D. Faddeev, Theor. Mat. Phys. (USSR) **4**, 745 (1971).

[29] D. Zwanziger, Phys. Rev. D**7**, 1082 (1973); Phys. Rev. Lett. **3 0**, 934 (1973); Phys. Rev. D1**1**, 3481 and 3504 (1975).

[30] Chung, V., "Infrared Divergence in Quantum Electrodynamics", Phys. Rev. **140B**, 1110-1122 (1965).

[31] T.W.B. Kibble, Phys. Rev. **173**, 1527; **174**, 1882; **175**,1624 (1968); J. Math. Phys. <u>9</u>, 315 (1968).

[32] Y. Zhang and P.H. Handel: "Derivation of the Non-Relativistic Propagator for Coherent Quantum 1/f Noise", *5th van der Ziel Symposium on Quantum 1/f Noise and Other Low Frequency Fluctuations in Electronic Devices*, AIP Conference Proceedings No. 282, P.H. Handel and A.L. Chung, Editors, pp. 102-104; See, e.g., J.S. Gradshteiyn and I.M. Ryzhik, Table of Integrals, Series and Products" Sec. 3.761, No. 9 and No. 7, Academic Press, New York 1965.

[33] P.H. Handel and D. Wolf, Phys. Rev. **A26**, 3727 (1982)

[34] P.H. Handel, C.M. Van Vliet and A. van der Ziel, "Derivation of the Nyquist-1/f Noise Theorem", <u>Proc. 7th Int. Conf. on Noise in Physical Systems and 3rd Int. Conf. on 1/f Noise</u>, Montpellier, May 17-20, 1983, M. Savelli, G. Lecoy and J.P. Nougier Editors, North Holland Publ. 1983, p. 93

[35] P.H. Handel, D. Wolf and K.M. Van Vliet: "Non Gaussian Amplitude Distribution of Thermal Noise in a resistor with 1/f Noise", <u>Proc. 6th Int. Conf. on Noise in Physical Systems,</u> P.H.E. Meijer, R.D. Mountain and R.J. Soulen Ed, NBS Special Publication 614, p. 196 (1981)

[36] P.H. Handel, "Instabilitäten, Turbulenz und Funkelrauschen in Halbleitern III; Turbulenz im Halbleiterplasma und Funkelrauschen". Z. Naturforschg.**21a**, 579-593 (1966).

[37] P.H. Handel, "Instabilities and Turbulence in Semiconductors", Phys. Stat. Sol. **29**, 299-306 (1968).

[38] X. Hu and P.H. Handel: "Fractal Dimension of a Simplified Quantum 1/f Noise Model", *5th van der Ziel Symposium on Quantum 1/f Noise and Other Low Frequency Fluctuations in Electronic Devices*, May 22-23, 1992, St. Louis, MO, AIP Conference Proceedings No. 282, P.H. Handel and A.L. Chung, Editors, pp. 119-123 (1993).

[39] See, e.g., J.L. Lumley, Stochastic Tools in Turbulence (Academic, New York, 1970), p. 48.

[40] R. Zuleeg and H.H. Wieder: Solid-State Electron. **9**, 657 (1966).

[41] Shu-Yau Wu: IEEE Trans. on Electron Dev. ED-**21**, 499 (1974); Ferroelectrics **11**, 379 (1976).

[42] Y. Higuma, Y. Matsui, M. Okuyama, T. Nakagawa and Y. Hamakawa: Jpn. J. Appl. Phys. **17**, 209 (1977).

[43] T.A. Rost, H. Lin and T.A. Rabsom: Appl Phys. Lett. **59**, 3654 (1991).

[44] K. Sugibuchi, Y. Kurogi and N. Endo: J. Appl. Phys. **40**, 2871 (1975).

[45] F. Schuermeyer, M. Shur, E. Martinez, and C. Cerny, Material Sci. and Engrg. **B28**, 264-267 (1994).

[46] B.R. Nag; *Theory of Electrical transport in Semiconductors*, Pergamon Press 1972, p. 111.

[47] S. Sinharoy, H. Buhay, M.H. Francombe and D.R. Lampe: Integrated Ferroelectrics **3**, 217-223 (1993).

[48] S. Ohmi, M. Yoshihara, T. Okamoto, E. Tokumitsu and H. Ishiwara: Jpn. J. Appl. Phys. **35**, 1254-57 (1996).

[49] P.C. Sun, Y.T. Mazurenko, W.S.C. Chang, P.K.L. Yu and Y. Fainman, Optics Lett. **20**, 1728 (1995).

[50] Y.T. Mazurenko, Appl. Phys. B **50**, 101 (1990).

[51] A.M. Weiner, D.E. Leaird, D.H. Retze and E.G. Paek, IEEE J. on Quantum Electron. **28**, 2251 (1992).

XI. PAPERS PUBLISHED DURING THIS GRANT

1. P.H. Handel: "Fundamental Quantum 1/f Noise in Small Semiconductor Devices", IEEE Trans. on Electr. Devices 41, 2023-2033 (1994).

2. P.H. Handel: "Subtraction of a New Thermo-Electrochemical Effect from the Excess Heat, and the Emerging Avenues to Cold Fusion", Proc. 4th Conf. on Cold Fusion, Maui, Hawaii, Dec. 1993, Electric Power Research Institute Press, 3412 Hillview Ave., Palo Alto, CA 94304, EPRI TR-104188, (July 1994), Vol. 2, pp. 7-1 to 7-8.

3. P.H. Handel: "1/f Noise Universality in High-Technology Applications", Proc. 1994 IEEE Internatl. Frequency Control Symp., June 1-3, 1994, Boston, MA, L. Maleki, Editor (Plenary Invited paper) IEEE Press, IEEE Catalog No. 94CH3446-2, Library of Congress No. 87-654207, pp. 8-21.

4. P.H. Handel and F.L. Walls: "Analysis of Quantum 1/f Effects in Frequency Standards", Ibid., pp. 539-540.

5. .V.A. Zhil'tsov, E.A. Manykin, E.A. Petrenko, A.A. Skovoroda, J.F. Leitner and P.H. Handel: "Spatially Localized Microwave Discharge in the Atmosphere", JETF, **81**, 1072 (1995). See also JETP **81** (6), 1072-1082 (1995).

6. P.H. Handel: " The Physical Meaning of the Quantum 1/f Effect as a Form of Quantum Chaos", *VI. van der Ziel Symposium on Quantum 1/f Noise and Other Low Frequency Fluctuations in Electronic Devices*, University of Missouri St. Louis, May 27-28, 1994, AIP Proceedings 371, P.H. Handel and A.L. Chung Editors, American Inst. of Physics Press, New York, 1996, pp. 45-48.

7. P.H. Handel and Y. Zhang: " A Bridge Between Coherent and Conventional Quantum 1/f Noise", Ibid., pp. 49-52.

8. P.H. Handel: "Discussion of the Conventional Quantum 1/f Noise Source Term: Quantum 1/f Effect in Frequency Standards", Ibid., pp 53-56.

9. P.H. Handel: "Coherent and Conventional Quantum 1/f Effect" Physica Status Solidi **b194,** pp. 393-409 (1996)

10.P.H. Handel: "Quantum 1/f Effect in Semiconductor Devices", Proceedings of the International NODITO Workshop, Brno, Czech Republic, July 18-20, 1995, J. Sikula and P. Schauer, Editors, pg. 30-38.

11. P. H. Handel: "Quantum 1/f Noise Theory and Experiment", Proc. 13th Int. Conf. on Noise in Physical Systems and 1/f Noise (ICNF'95), pp. 257-262, Palanga, Lithuania, May 29 - June 3, 1995; World Scientific Publishers, V. Bareikis and R. Katilius, Editor.

12. P.H. Handel and R. Zuleeg: "Application of High ε Paraelectric Materials to High-Transconductance HFETs with Low Noise and Low gate Current", Proc. of the Advanced Workshop on Frontiers of Electronics (WOFE '97), to be published.

13. P.H. Handel: "Two-Dimensional All-Optical Parallel-toSeries TDM and Demultiplexing by Spectral-Holographic Methods", Proc. of the Advanced Workshop on Frontiers of Electronics (WOFE '97), to be published.

14. P.H. Handel: "Negative Entropy In The Conventional Quantum 1/f Effect", Latest Results Paper, Proc. of the Advanced Workshop on Frontiers of Electronics (WOFE '97), to be published.

15. P.H. Handel: "Incoherence and Negative Entropy in the Quantum 1/f Effect of BAW and SAW Quartz Resonators", Proc. Frequency Control Symposium, Orlando, FL. May 28-30, 1997, to be published.

16. P.H. Handel: "Thermoelectric Excess Heat Effect in Electrolytic Cells", Zeitschr. für Physik B 95, 489-492 (1994).